Application of Nanofluids in Shell and Tube Heat Exchanger for Heat Transfer Enhancement

A Thesis Submitted

In partial fulfillment for the reward of the degree of

Master of technology

In Mechanical Engineering

SUBMITTED BY

BRIJBHUSHAN SINGH BIRMUWAN

(2K20/THE/O7)

UNDER THE GUIDANCE OF

PROF. B.B ARORA

DEPARTMENT OF MECHANICAL, PRODUCTION & INDUSTRIAL

AND AUTOMOBILE ENGINEERING

DELHI TECHNOLOGICAL UNIVERSITY BAWANA ROAD, DELHI-110042

CERTIFICATE

This is to certify that this report titled, "Application of Nanofluids in Shell and Tube Heat Exchanger for Heat Transfer Enhancement" being submitted by Brijbhushan Singh Birmuwan (Roll No. 2K20/THE/07) at Delhi Technological University, Delhi for partial fulfilment of the Degree of Master of Technology as per academic curriculum. It is a record of bonafide research work carried out by the student under my supervision and guidance, towards partial fulfilment of the requirement for the award of Master of Technology degree in Thermal Engineering. To the best of my knowledge this work is original as it has not been submitted earlier in part or full for any purpose before.

Prof. B.B Arora

(Supervisor)

Mechanical Engineering Department

Delhi Technological University, Delhi-110042

CANDIDATE'S DECLARATION

I, BRIJBHUSHAN SINGH BIRMUWAN(Roll No. 2K20/THE/07), hereby certify that the work which is being presented in this thesis titled "Application of Nanofluids in Shell and Tube Heat Exchanger for Heat Transfer Enhancement" is submitted in the partial fulfilment of the requirement for degree of Master of Technology (Thermal Engineering) in Department of Mechanical Engineering at Delhi Technological University is an authentic record of my own work carried out under the supervision of PROF. B.B ARORA. The matter presented in this report has not been submitted in any other University/Institute for the award of Master of Technology Degree. Also, it has not been directly copied from any source without giving its proper reference.

Signature of Student

ABSTRACT

Heating and chemical reactors benefit substantially from the serpentine tube arrangement in a tubular structure. Small space and high heat transfer coefficients may be achieved using the serpentine tube-in-tube design. ' An investigation of the effects of nanofluids, such as Al2O3/water and CuO/water nanofluids, on heat transfer (HT) and efficiency of a serpentine tube heat exchanger is the goal of this study. Modeling in Creo and CFD simulations are carried out using ANSYS's FLUENT software, respectively. When nanofluids are used, shell and serpentine heat exchangers become more effective and efficient. There is no additional pressure loss over serpentine heat exchangers owing to the ultra-fine particles and tiny volume fractions of nanofluid coolant. For low velocities, nanofluids have a greater impact, but for high velocities, the flow rate will take precedence.

KEYWORD: —CFD, ANSYS CFX, shell and tube, nanofluids.

ACKNOWLEDGMENT

I wish to express my profound gratitude and indebtedness to Prof. B.B ARORA, Department of Mechanical Engineering, Delhi Technological University, Delhi- 110042 for introducing the present topic and for his inspiring guidance, constructive feedback and valuable suggestion throughout the project work.

I am also thankful to Prof. S.K GARG, Head of Mechanical Engineering Department, Delhi Technological University, Delhi-110042 for his constant support and encouragement. I am also grateful to my seniors and classmates.

Lastly my sincere thanks to all my family and friends who has patiently extended all sorts of help for accomplishing this undertaking.

BRIJBHUSHAN SINGH BIRMUWAN

M.Tech (THERMAL ENGINEERING)

ROLL NO.:2K20/THE/07

TABLE OF CONTENT

LIST OF FIGURES

LIST OF TABLES

LIST OF ABBREVIATIONS

HE	Heat Exchanger
CFD	Computational Fluid Dynamics
NSE	Navier-Stokes Equation
HTC	Heat Transfer coefficient
FVM	Finite Volume Method

CHAPTER-1
INTRODUCTION

1.1 Introduction

The exchange of heat energy is part of a broad range of mechanical processes. Heat inclusion, expulsion, or movement has become a significant mechanical task throughout any contemporary workplace, beginning with one process stream and continuing to the next. A source of energy recovery and process liquid heating/cooling is provided by these techniques. It is possible to save energy, save process time, boost temperature evaluations, and extend the gear's service life by improving heating or cooling. The enhanced heat exchange (HE) activity even has a subjective effect on a few operations. Elite warm frameworks for heat exchange enhancement have been more popular in recent years. Some research has been done to better understand heat exchange execution for practical purposes such as heat exchange upgrading. As a result of the advent of high heat stream forms, there has been a surge in demand for novel heat exchange technology advances. There are a few ways to increase the efficiency of heat exchange. Expanded surfaces, vibration on heat exchange surfaces, and channels of a smaller size are just a few of the methods that may be used. The working liquid's heat conductivity may also be increased to increase heat exchange productivity. When compared to the warm conductivity of solids, common heat exchange liquids including water, ethylene glycol, and motor oil have relatively low warm conductivities. Solids with high thermal conductivity may be used to boost the warm conductivity of a liquid by dispersing small, dense particles into it. Several scientists have previously looked at the feasibility of using such suspensions of powerful particles with requested diameters of 2 millimeters or micrometers.

- The particles settle quickly, framing a layer at first glance and diminishing the heat exchange limit of the liquid.
- On the off chance that the course rate of the liquid is expanded, sedimentation is decreased, yet the disintegration of the heat exchange gadgets, pipelines, and so on., increments quickly.

- Especially when the cooling channels are narrow, the massive particle size tends to block upstream pathways.
- The weight drops in the liquid increments impressively.
- At long last, conductivity improvement given molecule focus is accomplished (i.e., the more prominent the molecule volume portion is, the more noteworthy the upgrade—and more prominent the issues, as demonstrated previously).

Consequently, the course of suspending particles in the fluid was a notable however dismissed alternative for heat exchange applications. Be that as it may, the rise of present-day materials innovation gave the chance to create nanometer-sized particles which are very unique from the parent material in mechanical, warm, electrical, and optical properties.

1.2 Nanofluids

Thermal properties of fluids assume a conclusive part in heating and additionally cooling applications in modern procedures. An important physical characteristic, thermal conductivity, determines how heat is exchanged between fluids. For ultra-high cooling applications, traditional heat exchange liquids have an inalienably weak thermal conductivity. For years, scientists have been looking for ways to increase the traditionally weak thermal conductivity of these common heat exchange liquids by adding strong chemicals, following the well-established successful medium theory (Maxwell, 1873) for stronger mix qualities. Because of the disadvantages, like low thermal conductivity, molecule sedimentation, consumption of segments of machines, molecule stopping up, extreme weight drop, and so on, calibration of these strong suspensions to the millimeter and micrometer ranges for improving heat exchange execution has failed. In the search for novel types of liquid suspensions with improved thermal characteristics and in addition heat exchange execution, molecule sizes were scaled down.

1.3 Applications of Nano Fluid

1.3.1 Industrial Cooling Applications

Routbort et al. [30] Using nanofluids for mechanical cooling was first proposed in 2008, which might outcome in considerable energy & emissions reductions. To govern 1 trillion

Btu of US industrial energy, nanofluids might replace cooling & heating water with nanofluids. More than 50,000–150,000 households might save 10–30 trillion Btu per year in U.S. electric power sector if nanofluids are used in closed-circuit cooling cycles. More specifically, emissions of carbon dioxide, nitrogen oxides, & sulfur dioxide would all be reduced by an estimated 5.6 million metric tonnes.

Han et al. [31] The fluids' effective thermal conductivity and specific warmth have both been improved by using phase transition materials like nanoparticles in nanofluids, simultaneously. A one-advance, the nano-emulsification process has been used to combine an indium nanoparticle suspension in poly alpha olefin (dissolving temperature, 157°C). A preliminary estimate was made of the fluid's thermophysical parameters, as well as their temperature dependence (temperature dependence). The fluid's effective specific heat was significantly boosted by the indium nanoparticles' observed dissolving and solidifying stages.

1.3.2 Smart Fluids

Clean energy resources, as well as the growing use of battery-powered gadgets like mobile phones and laptop computers, have made smart technology management of energy resources even more important. A new class of fluids known as nano-fluids can handle this energy demand and serve as smart fluids.

1.3.3 Nuclear Reactors

Kim et al. [32, 33] It has been determined that nanofluids, studied by the MIT Department of Nuclear Science and Engineering (NS&E), may help water-cooled atomic frameworks, which can only expel so much heat. Possible uses include pressurized water reactor (PWR) coolant, reserve security frameworks, quickening agent targets, plasma diverters, and so on [34]. [35] Nuclear power plants with pressurized water reactors (PWRs) use a method called basic heat flux (CHF) to limit the generation of steam. CHF occurs when vapor rises and covers the surface of the fuel bars rather than fluid water. To avoid the formation of a vapor layer surrounding the bar and thus significantly increasing the CHF, the fuel bars are coated with nanoparticles such as alumina using nanofluids rather than water. PWR is much more effective in tests at MIT's Nuclear Research Reactor, showing favorable results in the first

evaluations. Nanofluids might be utilized in extra cooling systems to rapidly cool down hot surfaces, producing a change in plant safety.

1.3.4 Extraction of Geothermal Power & Other Energy Sources

According to an MIT analysis, the total global geothermal vitality assets are estimated to be more than 13000ZJ (2007) . At present just 200ZJ would be extractable, be that as it may, with innovative upgrades, more than 2,000ZJ could be extricated & supply the world's vitality requirements for a few centuries. Nanofluids may be used to cool channels that are exposed to temperatures between 500 °C and 1000 °C while isolating vitality from the world outside. When drilled, nanofluids may be used to cool down equipment and gear that is subjected to intense friction and high temperatures. "Superconducting fluid" nanofluids might be used to separate vitality from the earth's center and produce a lot of work energy in a PWR control plant framework.

1.3.5 Nanofluid Coolant

A vehicle's mileage may be improved by reducing the amount of energy it takes to overcome twist obstacles. Around 65 percent of a truck's total power output is consumed by the streamlined drag while travelling at high speeds. To some extent this is correct, however this is owing to the big radiator that sits in front of the engine. Because nanofluids may be used as coolants, radiators can be smaller and put in better locations. As a result of the improved efficiency, coolant pumps may be reduced and truck motors can operate at higher temperatures while still fulfilling strict emission regulations since there is less fluid.

1.4 Heat Exchanger (HE)

This device is used to transfer heat between at least two fluids or between strong surfaces and fluids or between strong particles and fluids, at varied temperatures while in heated contact with each other. Outer heat and work interactions are rare in heat exchangers. Fluid heating and cooling, as well as the dissipation or accumulation of single or multicomponent fluid streams, are common uses. You may be cleaning, purifying, fractionating or distilling a fluid, or you may be attempting to recover or dissipate heat. The majority of heat exchangers use an isolating divider or dividers to transfer heat between fluids. Fluids in many heat exchangers

are separated by a heat exchange surface, so they don't mix or break apart in an ideal world. The term "instant exchange composition" or "basically recuperator" refers to these types of exchangers.

1.4.1 Shell and Tube Heat Exchangers

There are an array of round tubes inserted in tube shell with tube hub parallel to shell axis as shown in figure 1.1.1. Fluids flow in and out of the tubes in opposite directions. Frontend and backside heads and baffles are real components. Tubes (or tube bundles), shell, frontend and backend heads. They will be explained in more depth in the future. It's possible to use a wide range of internal developments in shell-and-tube exchangers, depending on your goals for heat exchange and weight drop and the strategies you use to reduce warm concerns and prevent spillages, make cleaning easier, keep working weights and temperatures in check, regulate consumption, and more. Additionally, DIN and other European and international standards are extensively utilised, along with ASME (American Society of Mechanical Engineers) evaporator and weight vessel rules, as well as the TEMA norms (TEMA, 1999). Using these classifications, shell-and-and-tube exchangers are categorised and designed.

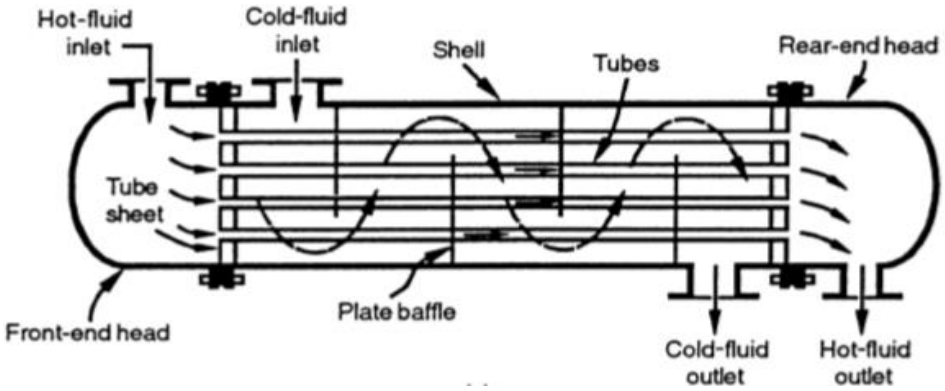

Fig. 1.1: BEM with a single shell and a single tube passage

TEMA standards must handle each of these complicated components, which specify the assembly resistances for different mechanical classes, the scope of tube diameters & pitches, baffling & bolster plates, weight classification, tube sheet thickness recipes, etc.

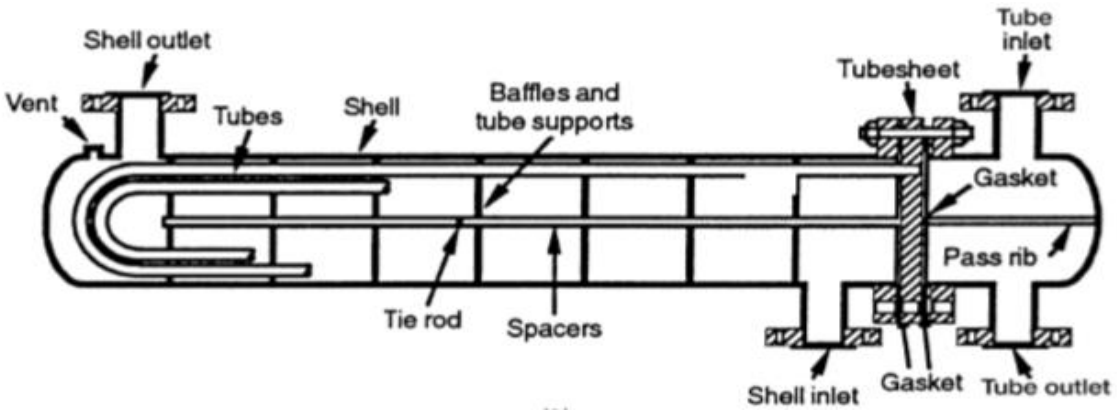

Fig. 1.2: BEU with a single shell passage and two tube passages

These heat exchangers employ round tubes from a variety of manufacturers. Straight and U-tube tube packs are the most common in exchangers in the process and power industries. Nonetheless, in cutting-edge atomic exchangers, sine-wave twist, J-shape, L-shape or hockey sticks, and upset hockey sticks are used to accommodate the tubes' significant heat development. Fig. 1.3 shows a section of the improved tube geometries seen in shell-and-tube exchangers. It is possible to use additional tube forms like helical and knife in the HX shell.

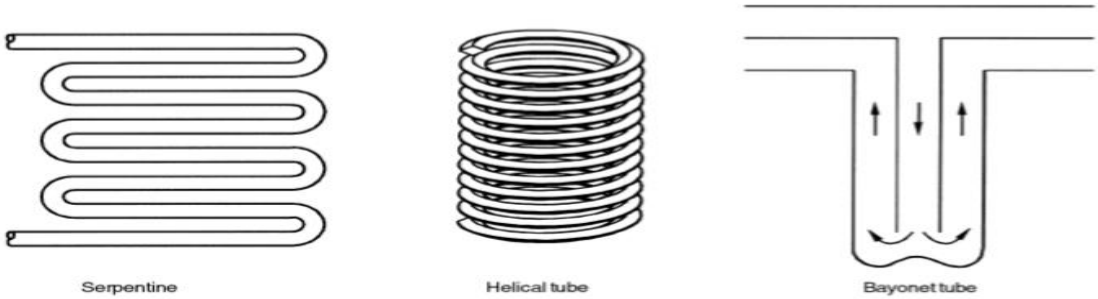

Fig. 1.3: Expansion of shell-and-tube exchanger tube configurations

Tubes with single dividers are utilised in many situations, however when dealing with radioactive sensitive, or noxious fluids and consumable water, twofold divider tubing is required. Tubes are exposed in many applications, however low-stature fins (low fins) are employed on the shell side when gas or a low-warm trade coefficient liquid is used. Modified low-fin tubing is also used in high-flux bubbling surfaces for the first time. Delivered in a thick-walled tube, they are usually essential fins. In accordance with the intended use, tubes are drawn, extruded or welded and provided in metals, plastics or ceramics.

CHAPTER-2
LITERATURE REVIEW

Rao et al. [1] The influence of factors like tube form and size, mass flow, intake temperature and pressure, and operation type on heat transfer (HT) & pressure drop was explored in study of heat exchangers utilising SCO2 as the working fluid. Additional information supplied included an overview of previous studies that looked at empirical heat transfer correlations prior to 2016.

Cabeza et al. [2]. A detailed examination of correlations and experimental studies done before to 2017 was used to establish HT coefficient (HTC) of SCO2 running in tubes of diverse geometries & diameters.

Ehsan et al. [3] A lack of unique universal association was discovered. Under turbulent flow conditions, previous experimental research on SCO2 in horizontal & vertical tubes were evaluated to determine HT properties & correlations of SCO2 in heating or cooling states. Additional considerations included pressure drop, buoyancy impact, heat transmission degradation, and wall temperature distribution in the discussion.

Baik et al. [4] For two different channel shapes, such as sharp corners and filleted corners, a series of CFD simulations were run by ANSYS CFX 14.5 and a PCHE-a precooler in SCO2 Brayton cycle. Water flows via cold channel, whereas SCO2 flows through hot channel. Pressure loss was 40% to 66% more in sharp corner channel than in surrounding corner channel.

Ren et al. [5] Simulated using ANSYS, the heat transport properties of SCO2 in the PCHE's horizontal semi-circular straight channel are examined Forced and mixed convective cooling abilities. In order to account for the thermal properties and buoyancy impact, a novel local HT coefficient correlation was devised.

Jiang et al. [6] Both 1D designs and dynamic models were made in Asper custom module for PCHEs in Brayton cycle. Because of this, it is possible to reduce the overall mass of the PCHE in the design model. The PCHE's dynamic model can forecast its short-term

behaviour. The findings demonstrated that PCHE has a quicker dynamic reaction than a standard shell-and-tube exchanger.

Marchionni et al. [7] The GT-SUITE programme was used to create 1D dynamic models of a SCO2 PCHE recuperator in order to simulate off-design performance & transient thermal events including startup, shutdown, and operating point shift. A 1D model may be used to forecast SCO2 PCHE recuperator performance, indicating that the stat-up process should be watched.

Ma et al. [8] The dynamic model of a SCO2 PCHE was established using 3D CFD simulations in different operating situations. The PCHE's thermal and hydraulic performance was then estimated using a neural network trained on a variety of operating factors.

Guo and Huai et. al. [9]Heat exchanger is separated into many subheats along the major flow channel in the technique. One sub-heat exchanger has a constant thermo-physical parameter, although they differ from one another. The 1D HT balancing equations are made among primary & secondary fluxes. Simple numerical procedures are used to solve the equations after all of the variables have been determined. Design and dynamic modelling of SCO2 heat exchangers in response to changing operating conditions might benefit from the technique. Now it's possible to use this technique on SCO2 PCHEs with flat channel wires as well!

Li et al. [10] The overall thermal performance of SCO2 PCHE was briefly discussed in terms of a preliminary approach to taking input pressure and temperature into account. HTC U & dimensionless pseudocritical point temperature Tb/Tpc form the basis of this method. To be sure, it is not a perfect starting place for creating new methods, but it is a decent first step toward using this methodology in project of SCO2 heat exchangers in future despite its limitations.

Eter et. al. [11] The heat transfer in CO2-cooled tubes with & without flow barriers was studied at a supercritical pressure of 7.69–8.36 MPa, a mass flow rate of 200–1184 kg/m2 s, and a heat flux of 1–175 kW/m2. The most efficient heat transfer barriers were flow obstruction and a short pitch.

Nascimento and Garcia et. al. [12] Small square protrusions were added to walls of flat tubes to facilitate HT in small heat exchanger. According to findings, heat transfer was increased by a factor of 1.37 to 2.28 when using shallow square protrusions.

Manoram et al. [13] The use of dimpled tubes in the heat exchange system was simulated to enhanced collector's HT rate and thermal efficiency. For 2.5 kg/min mass flow, a friction factor increases of 11.1% was measured in the dimpled tube against a plain tube, by a pitch to dimple diameter ratio ranging from three to six dimples in between two pitches.

Sahu and Prasad et. al. [14] Arc-shaped wire rough elements were used to investigate thermal performance of air collectors used for heating. An arc-shaped wire roughened solar air heater performed better at all Reynolds numbers.

Thangamuthu et al. [15] An external microprocessor pack with a multi-walled CNT & graphene layer was subjected to heat transfer testing. Heat transfer efficiency increased by 16 and 20 percent and surface temperature decreased by 7 and 9 degrees Celsius as compared to an equivalent external microprocessor pack without the coating. The multi-walled CNT coating does not demonstrate as good a heat transfer behaviour as the Graphene Nano sheet because it connects strongly between individual sheets.

Bonanno et al. [16] Al2O3 nanoparticle sol deposition was used to study heat transfer in finned heat exchangers with a hydrophobic nano-coating. Uncoated heat exchangers' heat transfer coefficients were as low as 116.46 W/m2 K, whereas coated heat exchangers' coefficients were higher at 176.47 W/m2.

Meikandan et al. [17] To further understand the impact of CNT coating on HT coil surface while exposed to air flow, an experiment was conducted. As the CNT coating is used, surface area of tube is increased by 46% when compared to the bare tube area. According to the research, the Nano coating had no effect on drag but did increase heat transfer rate by 24.2%. The coated heat exchanger also had a better transient temperature response.

Kumar et al. [18] Heat exchanger fins were coated with MgZrO8 and Ni–Cr alloy nanocoating materials. Compared to an exchanger coated with a Ni–Cr alloy, the MgZrO8-

coated one has a higher HT (Kt). An suitable nanomaterial for covering heat exchangers is MgZrO8.

Ali et al. [19] A heat transfer enhancement method's effectiveness or gain may also be applied to assess its efficiency. Enhancement efficiencies in smooth and enhanced tubes are determined using this expression:

$$\eta = \frac{Nu/Nu_0}{f/f_0}$$

With regard to an enhanced approach, illustrates how much heat transfer improvements are offset by an increase in friction factor. Improved methods are associated with higher values. Dimples, protrusions, twisted tape inserts, and other rough components are shown to have an effect on the friction factor ratio f /f0.

Jadhav et al. [20] Passive heat transmission technologies including dimples, protrusions, twisted tape inserts, abrasive components, and nano-coatings do not need external energy. Instead than relying on external power to keep the augmentation process going, passive approaches don't need as much technical expertise.

Chai and Tassou et. al. [21] The roughness of the surface is raised as a consequence of the use of dimples, protrusions, and other rough components to growth HT area & HTC. There is reduced hydraulic loss when using dimple and protrusion techniques as compared to rough element approaches at same degree of HT enhancement.

CFD simulations will be used to analyse and optimise the heat exchanger's primary dimensions and geometrical form. In [22,23] and for shell-and-tube, microchannel, & plate-fin HT & so on, CFD simulation-based optimization examples have been presented. Based on a number of CFD simulations, a surrogate model [24] or response surface model [25] is created. ANSYS Workbench has provided a suitable setting for this.

The preliminarily designed heat exchanger may be improved by reducing the objective function, such as the rate of entropy formation, exchanger weight, effectiveness, operating

cost or any combination of these. An optimization approach, 1D heat transport models, and an optimization strategy are all presented in-depth in the scholarly work. [26,27,28,29,30,31]

Mishra et. al. [32] One example is a micro-channel or plate heat exchanger, although there are other instances of a shell and tube HT. A number of empirical and correlational correlations need to be revised since the fluids in these studies are based on continuous thermo-physical and transport properties

CHAPTER-3

COMPUTATIONAL FLUID DYNAMICS

3.1 Concept of Computational Fluid Dynamics:

These computations are used to model the interaction of liquids and gases with boundaries specified by boundary conditions. A higher level of performance may be attained by using powerful, high-speed supercomputers.

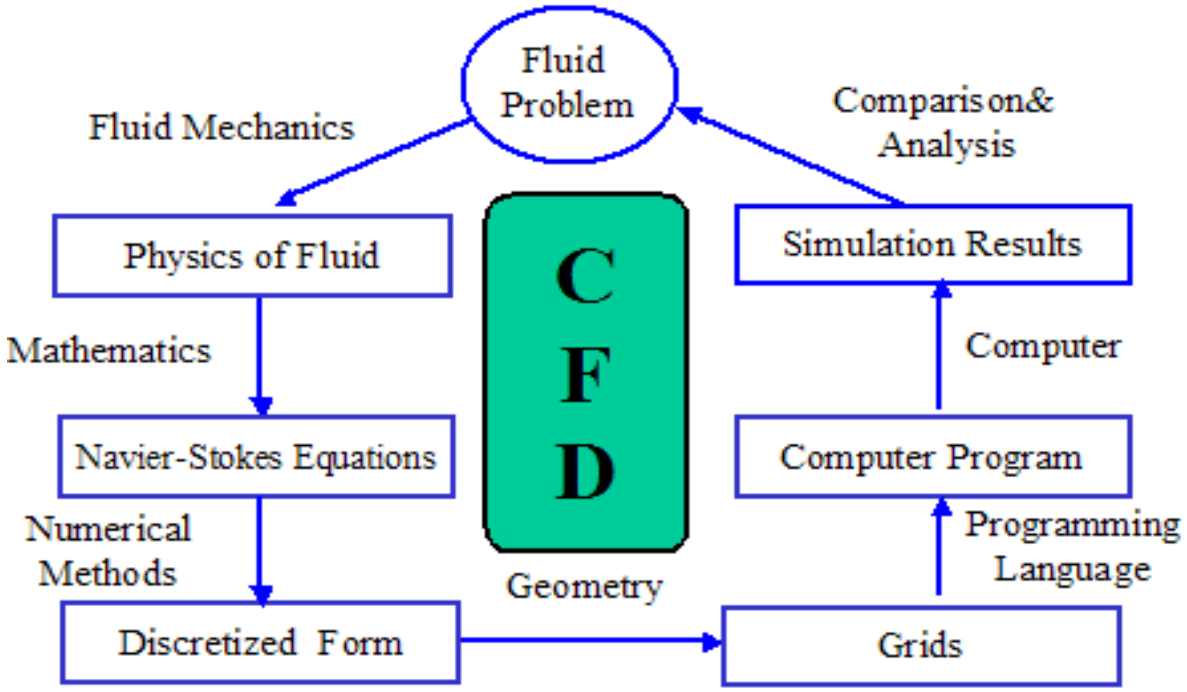

Fig. 3.1: Process of Computational Fluid Dynamics

The Navier-Stokes Equation, which serves as the governing equation of CFD, describes the physical characteristics of fluids. Finite Difference and Finite Volume techniques are used to discretize these equations in order to solve them on a computer. Programming languages like C and Fortran are used to break down the domain into smaller subdomains. Using RMS residual graphs, the computer iteratively solves the equations and minimises error. ANSYS, Flotran, Flow therms, and Open Foam are just a few of the many CFD solvers now available on the market.

3.2 Importance of Computational Fluid Dynamics

Theoretical, experimental, and simulation-based approaches may all be used to better understand fluid flow. Table 3.1 shows the benefits of CFD over experimental methods.

Table 3.1: The Simulation vs. Experiment Debate

	Simulation (CFD)	Experiment
Cost	Cheap	Expensive
Time	Short	Long
Scale	Any	Small/Middle
Information	All	Measured Point
Repeatable	Yes	Some
Safety	Yes	Some Dangerous

3.3 Application of Computational Fluid Dynamics

With numerous advantages CFD finds its application in industries such as heat ventilation, aeronautics, air conditioning, hydraulics and power generation etc

3.3.1 Physics of Fluid

For incompressible fluid like water in which density is distinct as mass per unit volume.

$$\rho = \frac{M}{V}\frac{kg}{m3} \qquad (3.1)$$

The viscosity is an internal characteristic of a fluid that opposes flow.

$$\mu = \left[\frac{Ns}{m^3}\right] = [\text{Poise}] \qquad (3.2)$$

Table 3.2: Show densities & viscosities of air, water and honey.

Substance	Air (18ºC)	Water (20ºC)	Honey (20ºC)
Density (kg/m^3)	1.275	1000	1446
Viscosity (P)	1.82e-4	1.002e-2	190

1) **Conservation Law**

According to the Navier Stokes Equation, that is built on conservation of mass, momentum & energy in computational fluid dynamics (CFD).

Mass change in any domain is given by

$$\frac{dM}{dt} = \dot{m}_{in} - \dot{m}_{out} \qquad (3.3)$$

If $\dot{m}_{in} - \dot{m}_{out} = 0$

We have

$$\frac{dM}{dt} = 0$$

Which means

$$M = \text{const}$$

3.3.2 Navier-Stokes Equation (NSE)

Mass, momentum & energy conservation may be used to generate continuity, momentum and energy equ.

1) **Continuity Equation**

$$\frac{Dp}{Dt} + \frac{\rho \partial U}{\partial x} = 0 \qquad (3.4)$$

2) **Momentum Equation**

$$\frac{\rho\, \partial U}{\partial t} + \frac{\partial U}{\partial x} = -\frac{\partial P}{\partial x} - \frac{\partial \tau}{\partial x} + \rho g \qquad (3.5)$$

Where

$$\tau_{ij} = -\mu\left(\frac{\partial U}{\partial x} + \frac{\partial U}{\partial x}\right) + \frac{2}{3}\delta\mu\frac{\partial U}{\partial x} \quad (3.6)$$

I: Local change with time

II: Momentum convection

III: Surface force

IV: Molecular-dependent momentum exchange (diffusion)

V: Mass force

3) Energy Equation

$$\frac{\rho c \partial T}{\partial t} + \frac{\rho c U \partial T}{\partial x} = -\frac{P \partial U}{\partial x} + \frac{\lambda \partial T}{\partial x 2} - \frac{\tau \partial U}{\partial x} \quad (3.7)$$

I: Energy change with time (local)

II: Convective term

III: Pressure work

IV: Heat flux (diffusion)

V: Irreversible transfer of mechanical energy into heat

3.3.3 General Form of NSE

NSE can be rewritten in simplified form as

$$\frac{\partial(\rho\phi)}{\partial t} + \partial/\partial x(\rho U\phi - \partial\emptyset/\partial x) = q \quad (3.8)$$

3.4 Finite Volume Method

A logical set of circumstances, the Navier-Stokes conditions must exist. Despite the fact that they may be comprehended and illuminated by humans, they must be reduced to a discretized form if they are to be understood by a computer. Discretization is the term used to describe this process. The normal discretization techniques are limited distinction, limited component and limited volume strategies. Here we present limited volume technique.

3.4.1 The Approach of Finite Volume Method

Navier stokes equation can be integrated over control volume & by application of Gauss theorem we get

$$\int \frac{\partial}{\partial x} \Phi dV = \int \Phi . ndS \qquad (3.9)$$

Integral form of NSE is

$$\int \frac{\partial(\rho\Phi)}{\partial t} dV + \int \left(\rho U\Phi - \frac{\partial\Phi}{\partial x}\right) . ndS = \int q dV \qquad (3.10)$$

By multiplyVariables are kept at the control volume's centre, therefore getting to the surface variables involves interpolation. Two kinds of interpolation procedures exist: upwind interpolation and central interpolation; each has its advantages and disadvantages.ing the volume & value at control-volume centre, we may estimated volume integral. Fig 2.2 shows a two-dimensional domain. P's control volume has a mass and momentum that we can estimate using a formula.

$$\text{m}=\int \rho dV \text{ , mu } = \int \rho u dV \qquad (3.11)$$

Surface integral can be approximated, for example pressure force, we have

$$\int P dS = \sum P . S \qquad (3.12)$$

Variables are kept at the control volume's centre, therefore getting to the surface variables involves interpolation. Two kinds of interpolation procedures exist: upwind interpolation and central interpolation; each has its advantages and disadvantages.

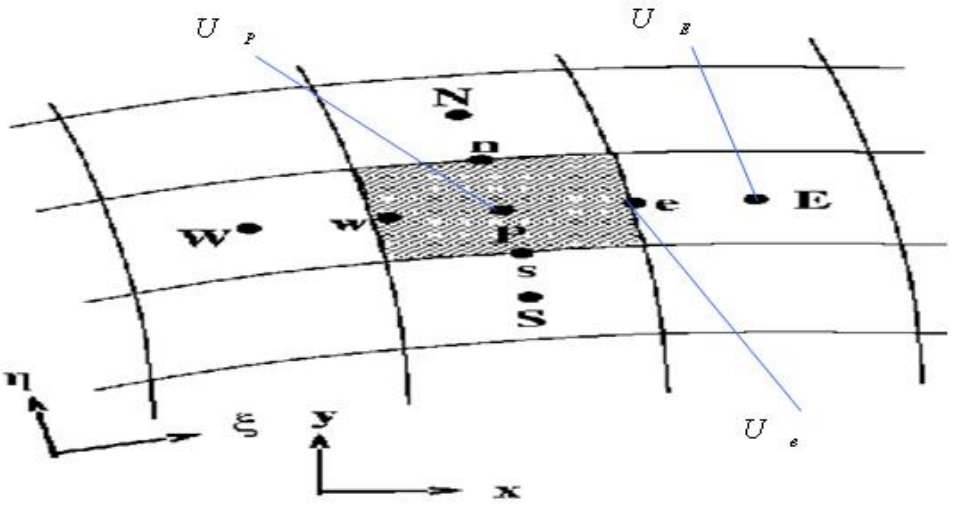

Fig. 3.2: 2D Structured Grid Domain

1) Upwind Interpolation

$$U_e = \begin{cases} U_P & \text{if } (\vec{U}\cdot\vec{n})_e > 0 \\ U_E & \text{if } (\vec{U}\cdot\vec{n})_e < 0 \end{cases} \qquad (3.13)$$

2) Central Interpolation

$$UE = UE\lambda + Up(1-\lambda) \qquad (3.14)$$

3.4.2 Conservation of Finite Volume Method

To deal with the discretized NSE using finite difference and finite element methods, we must physically manage the preservation of mass, force, and vitality. Navier-Stokes conditions are naturally satisfied in each control volume if the Navier-Stokes condition is met in all the control volumes. As a result, if each control volume's preservation is met, the whole space will be met. In computational fluid dynamics, finite volume is preferred because of this reason.

3.5 Grids

Grids are offered in three distinct varieties i.e structured grids, unstructured grids and block structured grid (fig 3.3). In this form of grids have identical no. of components surrounding it

which can be expressed and stored simply. Unstructured grids may be utilised for domains with a lot of complexity. E.g., fig 3.4 is an airfoil. The construction of airfoil is quite complicated, flows in the vicinity of object is complex and necessitates finer grid. Locations away from airfoil where flow is comparably simple coarse grid can be used. It is very popular in CFD.

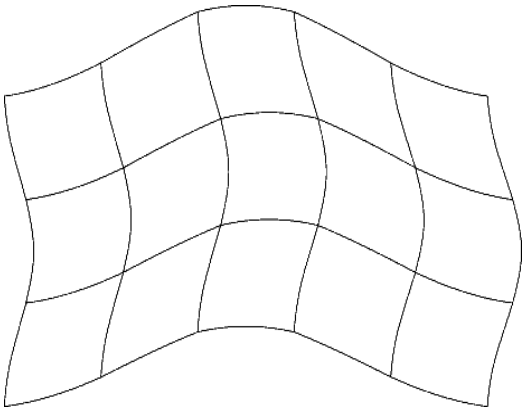

Fig. 3.3: Structural Layout

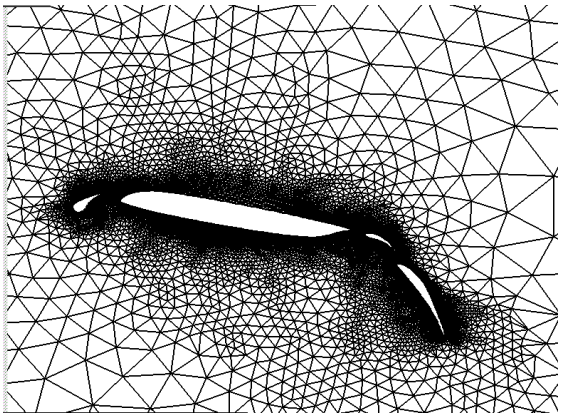

Fig. 3.4: Unstructured layouts

3.6 Boundary Condition

When solving equation systems, boundary conditions like no-slip, axisymmetric, inlet- and outlet-boundary, and periodic are often used. Fig 3.5 gives an example of flow across pipe. The boundary conditions are defined for left face as inlet, right face as outlet to keep all properties constant, no slip on, wall is defined with zero velocity which is no-slip boundary condition. At centre of pipe, we may use axisymmetric boundary condition.

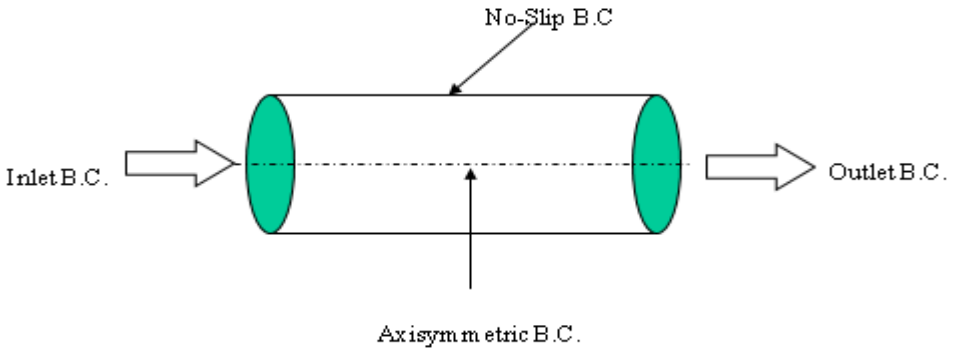

Fig. 3.5: Inlet and outlet boundary conditions

CHAPTER-4

RESEARCH GAP AND OBJECTIVES

4.1 Research Gap

Previous researches were focused on design optimization of shell & tube h HEs which included baffling arrangement and inclination angles using experimental and CFD simulation techniques. Some researches were focused on application of nano fluids as coolant in shell and tube HEs but presently application of nano fluids in shell and serpentine heat exchanger requires investigation.

4.2 Objectives

Nanofluids, such as Al2O3/water and CuO/water nanofluids, are being used in this study to examine their influence on the HT rate and efficiency of heat exchangers utilising serpentine tubes in tube configuration & to compare findings with water as fluid.

1) CAD modelling of the shell and serpentine heat exchanger.
2) Performing CFD analysis using ANSYS CFX solver.
3) Analyzing heat exchanger using water as fluid.
4) A heat exchanger's efficiency may be determined by determining its heat transfer coefficient (HTC).
5) Changing fluid to CuO/water and determining heat transfer coefficient, effectiveness of heat exchanger.
6) Drawing comparison using graphs and tables.

4.3 Properties of Nano Fluid

Selection and assessment of nanofluid thermophysical characteristics are critical to nanofluid applications. The thermophysical characteristics of nanofluids are calculated using the single-phase approach. The nano fluid under consideration in this work is a water-based combination that contains mostly CuO.

Table 4.1: Properties of nano fluid (CuO/water)

MATERIAL	DENSITY (Kg/m^3)	SPECIFIC HEAT(J/Kg.K)	THERMAL CONDUCTIVITY (W/m.K)	DYNAMIC VISCOSITY Kg/m.s
PURE WATER	981.3	4189	.643	.000598
CuO(1%)-water	1061	4150.9	.662	.000612
CuO(2%)-water	1140.7	4112.8	.682	.000627
CuO(3%)-water	1220.4	4074.8	.702	.000642
CuO(4%)-water	1300.2	4036.7	.723	.000657
CuO(5%)-water	1378	3998	.744	.000672

Table 4.2: Properties of nano fluid (Al_2O_3 water)

MATERIAL	DENSITY (Kg/m^3)	SPECIFIC HEAT(J/Kg.K)	THERMAL CONDUCTIVITY (W/m.K)	DYNAMIC VISCOSITY Kg/m.s
PURE WATER	981.3	4189	.643	.000598
Al_2O_3 - water C=1%	1007.4	4154.7	.661	.000612
Al_2O_3 - water C=2%	1033.6	4120.5	.68	.000627
Al_2O_3 - water C=3%	1059.8	4086.2	.699	.000642
Al_2O_3 - water C=4%	1086	4052	.719	.000657
Al_2O_3 - water C=5%	1112.2	4017.8	.739	.000672

CHAPTER-5

METHODOLOGY

5.1 Flowchart

A flowchart depicting the steps required in analysing a shell and serpentine heat exchanger is shown below.

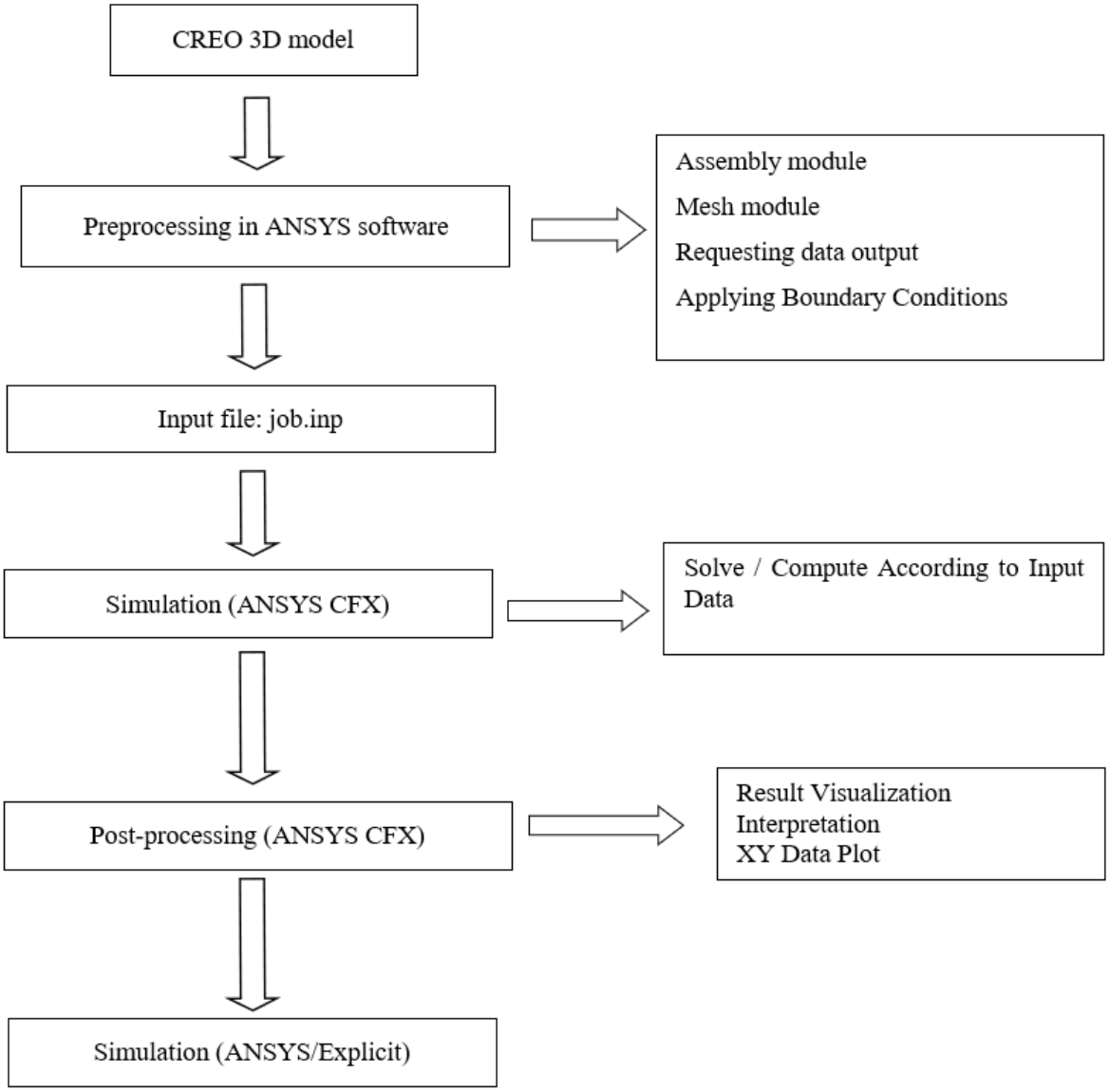

Fig.5.1: Methodology Flowchart

5.2 CAD Modeling

Creo 2 software is used to create a CAD model of the shell & serpentine HEs in accordance with the dimensions shown in table 5.1. A CAD model is created by modelling and assembling individual parts. There is a bidirectional associativity and parent/child link between Creo and other parametric 3D modelling tools made by PTC.

Table 5.1: Dimensions of shell and serpentine heat exchanger

HEAT EXCHANGER LENGTH	1300mm
SHELL OUTER DIAMETER	200mm
SHELL THICKNESS	3.2mm
TUBE OUTER DIAMETER	30mm
TUBE THICKNESS	1.5mm
NUMBER OF SERPENTINE TUBE	1

STEP 1: Part model of shell is modeled using extrude, sketch tool as shown in fig 5.2 below using front and top planes along with inlet and outlet of coolant.

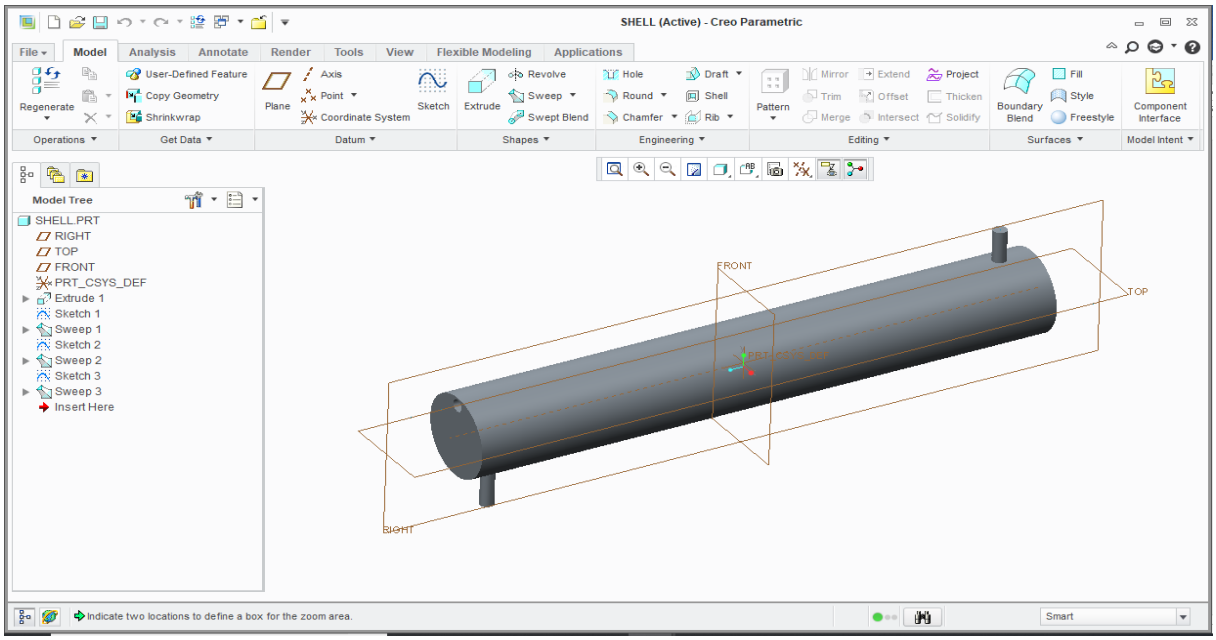

Fig. 5.2: Sketch of computational domain

STEP 2: Using sweep and sketch tool serpentine tube is modeled as shown in fig 5.3 below using front and right plane of part modeler.

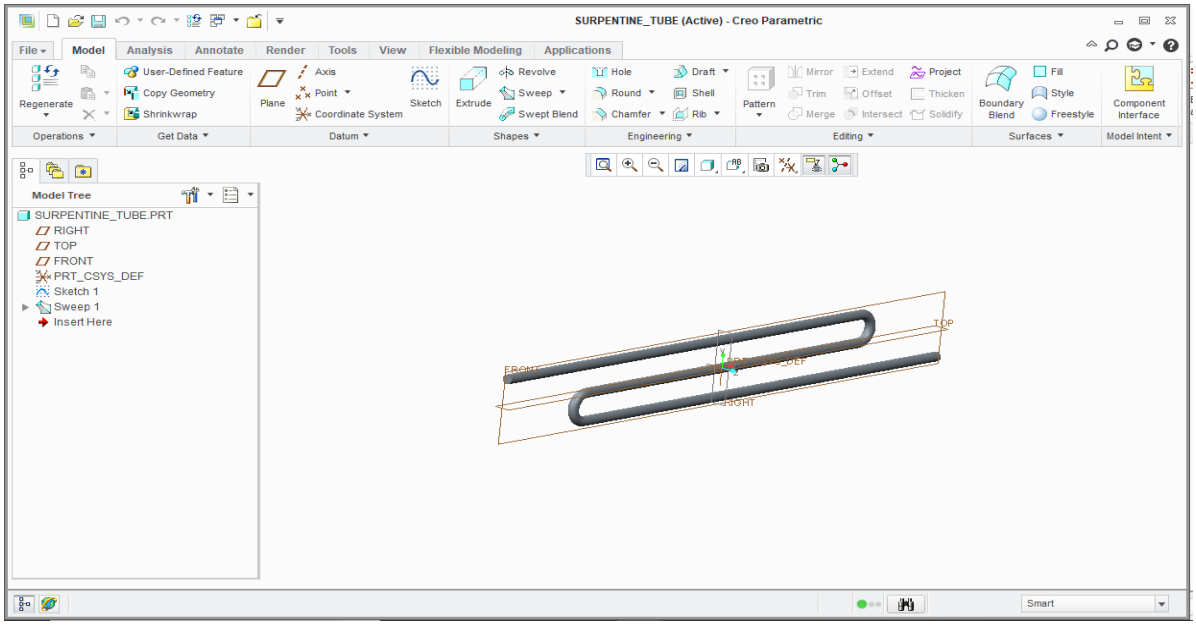

Fig. 5.3: Serpentine tube model

STEP 3: Tube coating is modeled applying sketch and sweep tool as exposed in fig 5.4 below using front plane of part modeler.

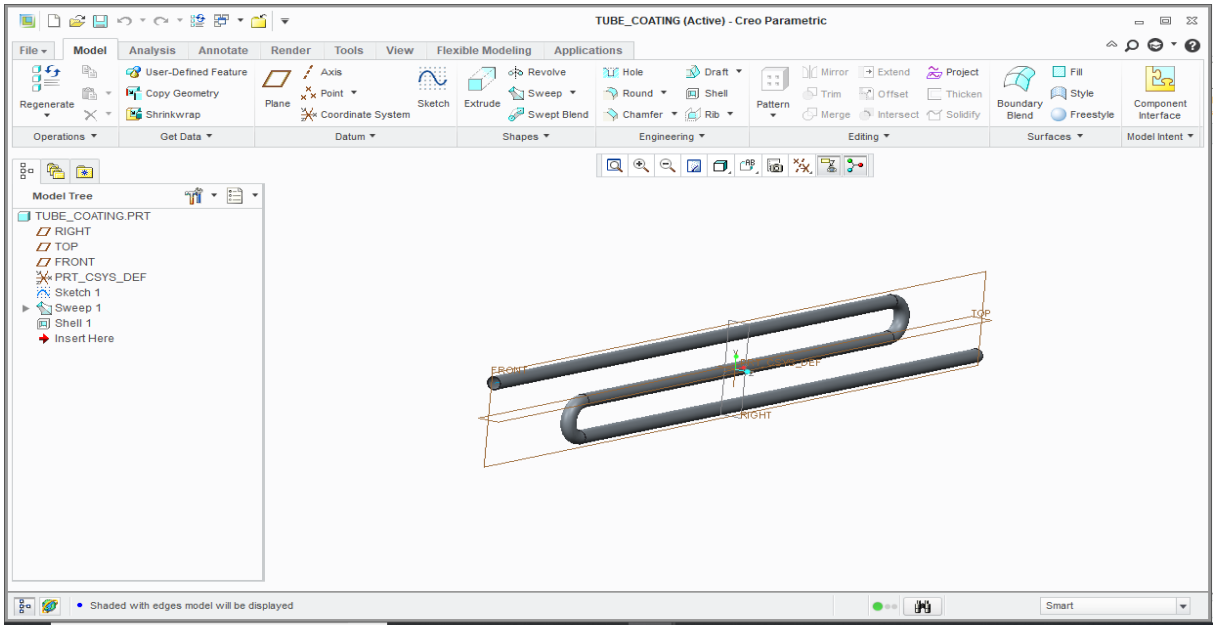

Fig. 5.4: Tube coating

STEP 4: Shell and serpentine tubes are assembled using coincident and distance constraints in front and top plane.

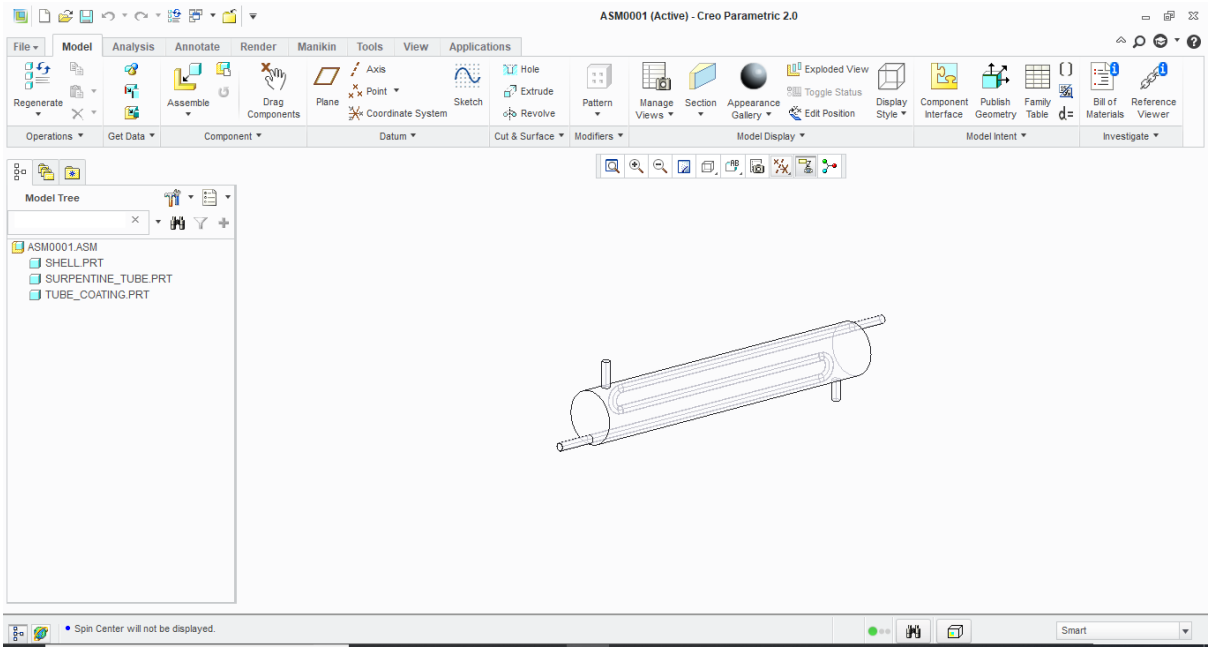

Fig. 5.5: Assembly modeling

5.3 CFD Simulation Using Ansys

STEP 1: A CAD model is imported into the workbench using an import tool, and other tools are used to clean up the geometry.

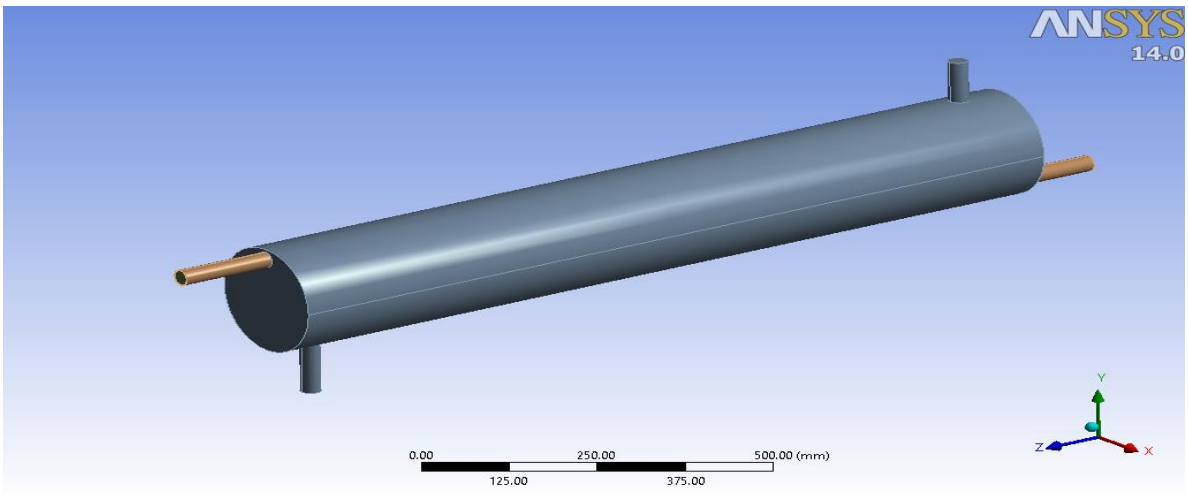

Fig. 5.6: Imported CAD model in ANSYS

Creo CAD model is exported in iges format, allowing it to be used with a variety of additional design and analysis tools. Hard edges, gaps, and other imperfections need to be fixed using cleanup tools.

STEP 2: Brick components are used in the model's meshing, together with provided parameters and mesh density. An inflation rate of 100 percent is used to adjust the mesh size and inflation to normal. Slow, medium, and fine transitions and smoothing are selected, as is a span angle of around 30 degrees.

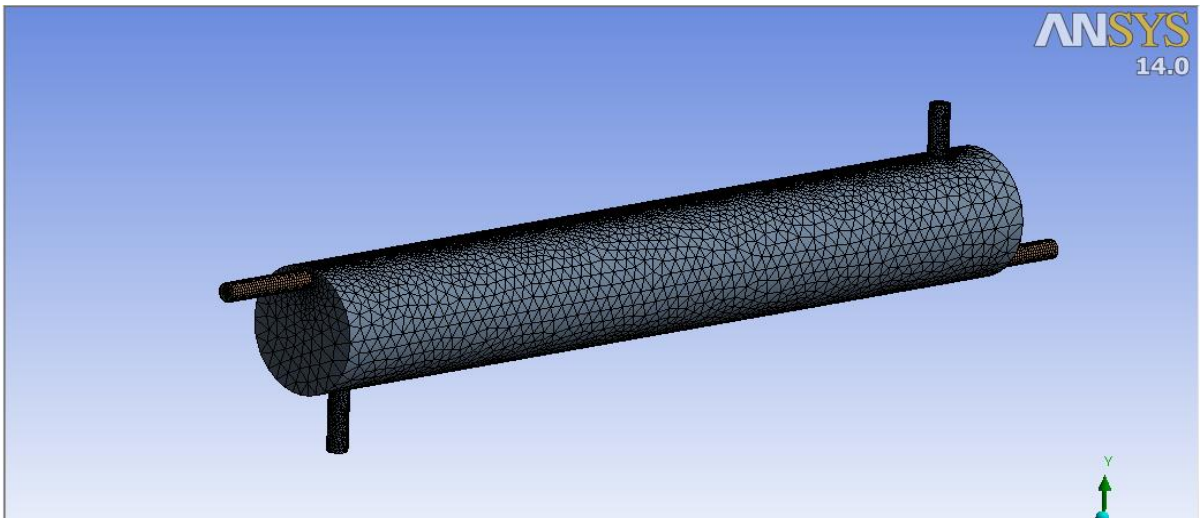

Fig. 5.7: Imported CAD model in ANSYS

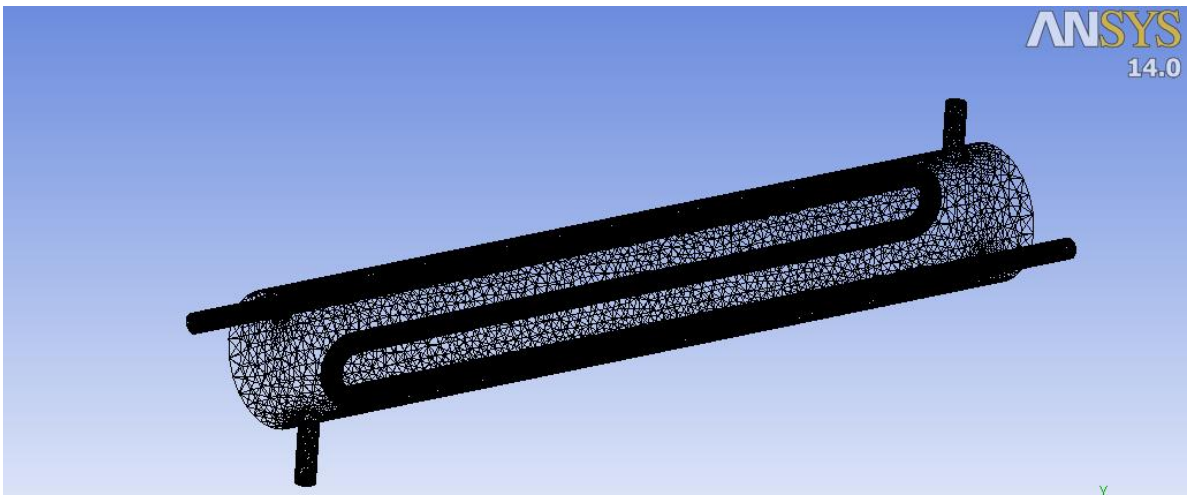

Fig. 5.8: Wireframe meshed model in ANSYS

Statistics	
Nodes	201623
Elements	622079
Mesh Metric	None

Fig. 5.9: Number of nodes and elements in mesh

STEP 3: For shell, tube, and tube coating, there are three distinct domains. It is set to fluid, water, and nanofluid for further analysis. The reference pressure for the shell domain is 1 atm, & turbulence model is set to k-epsilon. One percent, two percent, three percent, four percent, and five percent

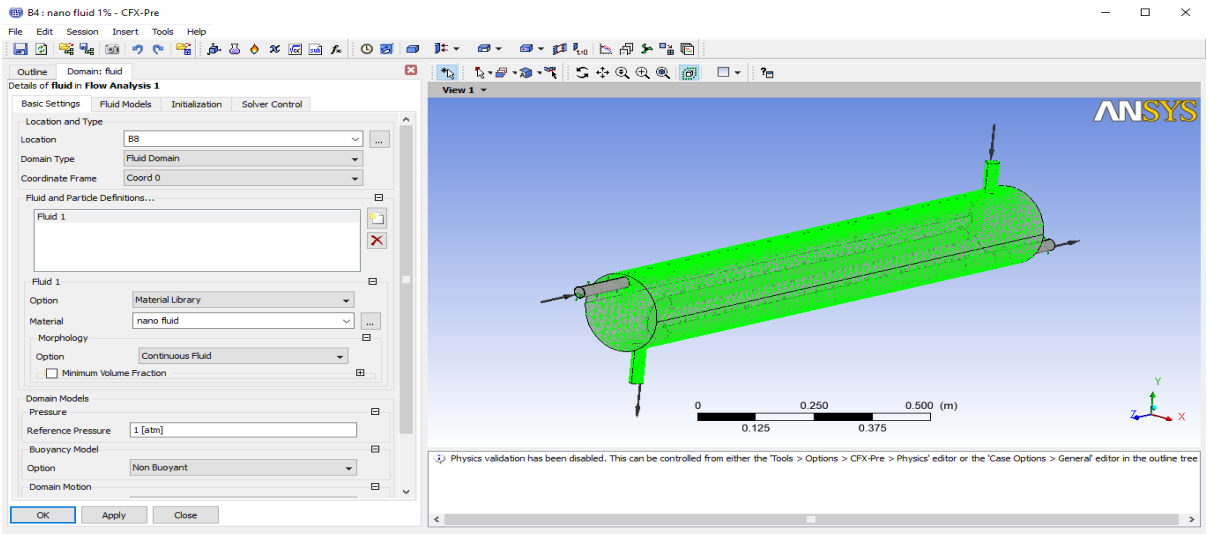

Fig. 5.10: Fluid domain

As illustrated in fig. 5.11 below, the tube domain is distinct as a fluid domain with water as the material.

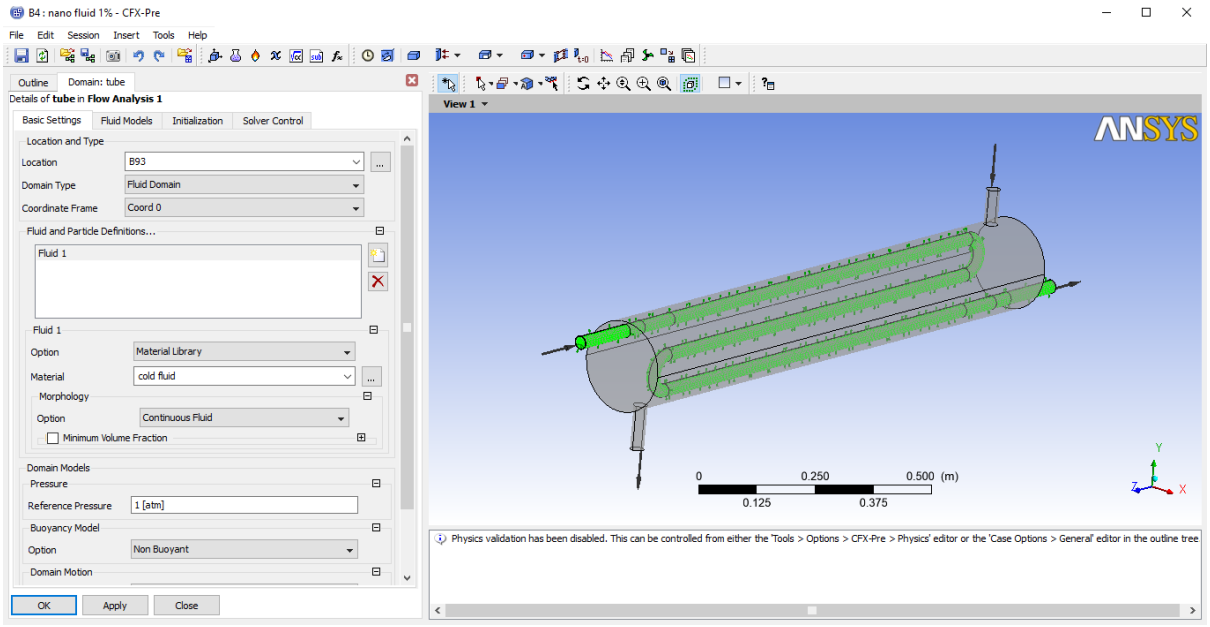

Fig. 5.11: Tube domain

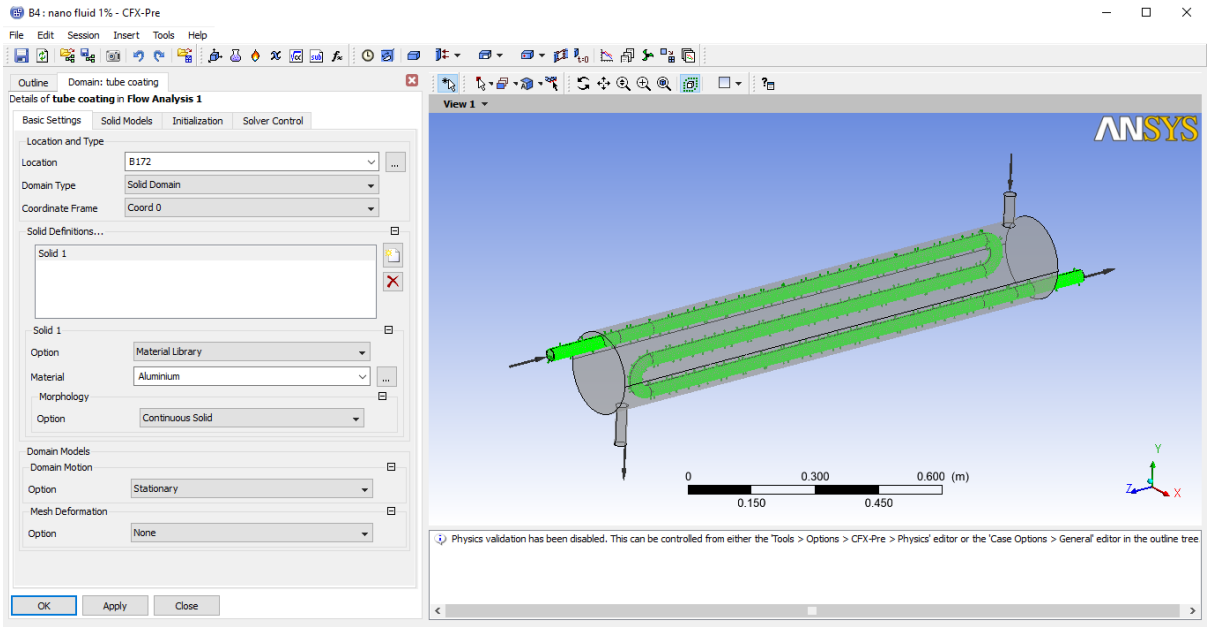

Fig. 5.12: Tube coating domain

Fig 5.12 shows that tube coating is a solid domain using aluminium as the material.

STEP 4: The inlet and outlet definitions used to establish boundary conditions are presented below. A mass flow rate of.04 kg/sec and a temperature of 365 K are used to define the intake. The turbulence is set at a medium level, or 5% of the maximum.

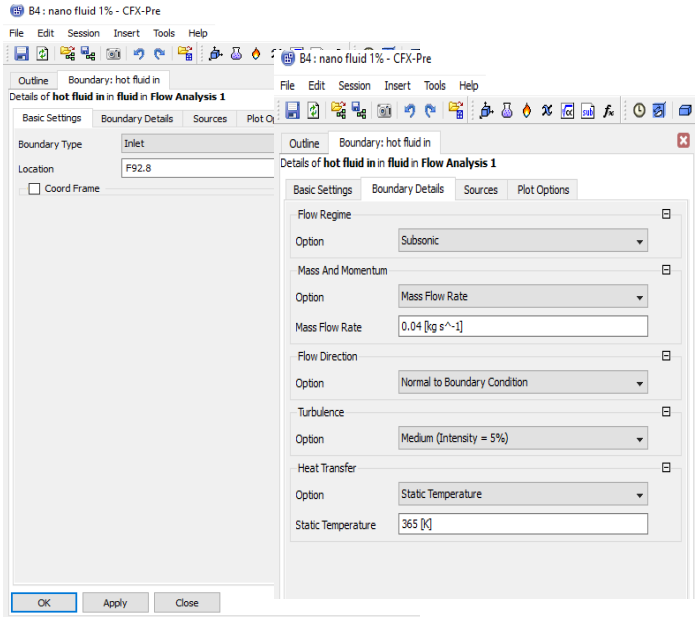

Fig. 5.13: Definition of the inlet for hot fluid

Figure 5.14 shows the flow rate of 0.05 kg/sec and the temperature of 300K, with the turbulence severity set to medium at 5%.

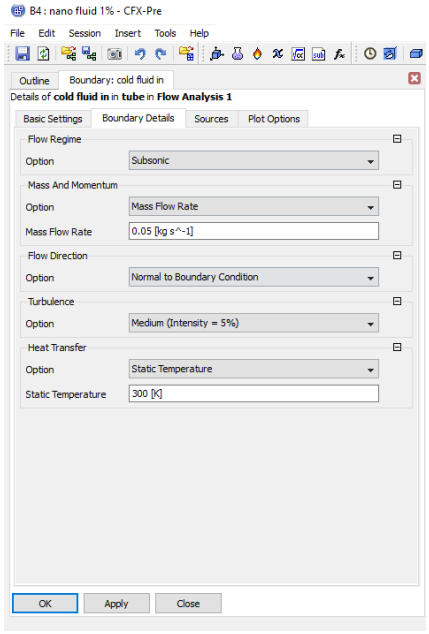

Fig. 5.14: Inlet definition for cold fluid

STEP 5: For tube and tube coating, two fluid-solid interfaces are designed, with a conservative interface heat flux to enable heat transmission across two media. To transmit

heat between two different media, a similar interface is constructed for tube coating and hot fluid.

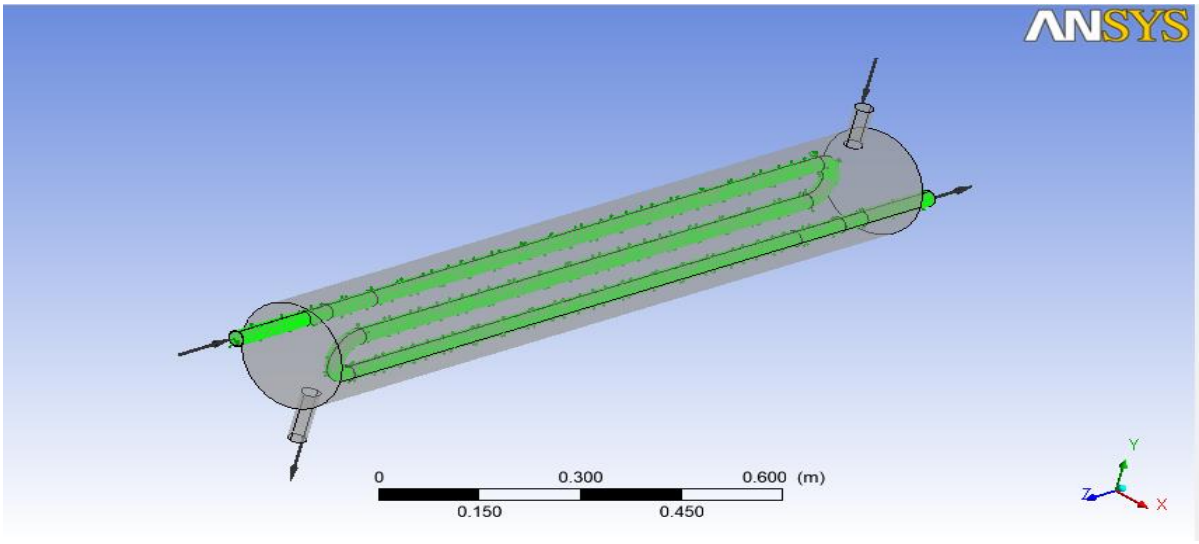

Fig. 5.15: Fluid solid interfaces

STEP 6: Both the RMS residual plots as well as the number of iterations have been set to 1e-5 in the Solver control parameters. The number of iterations has been set to 100. The timescale factor of 1 is used in this situation.

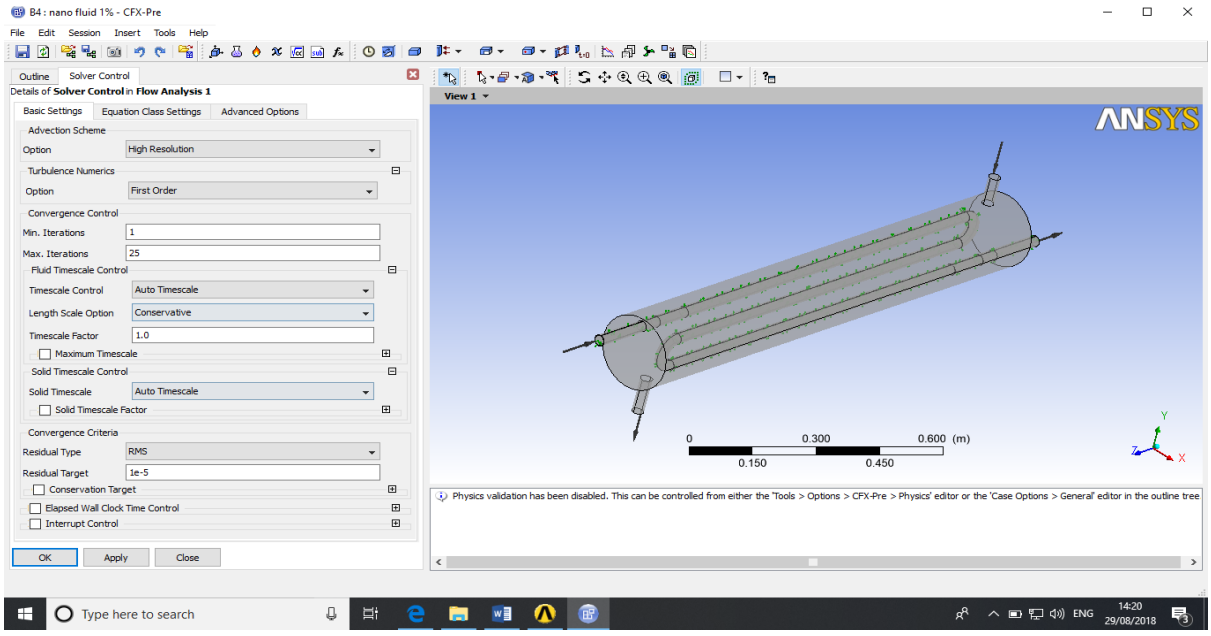

Fig. 5.16: Solver settings

STEP 7: For each of the input variables, the solver generates a set of RMS residual graphs.

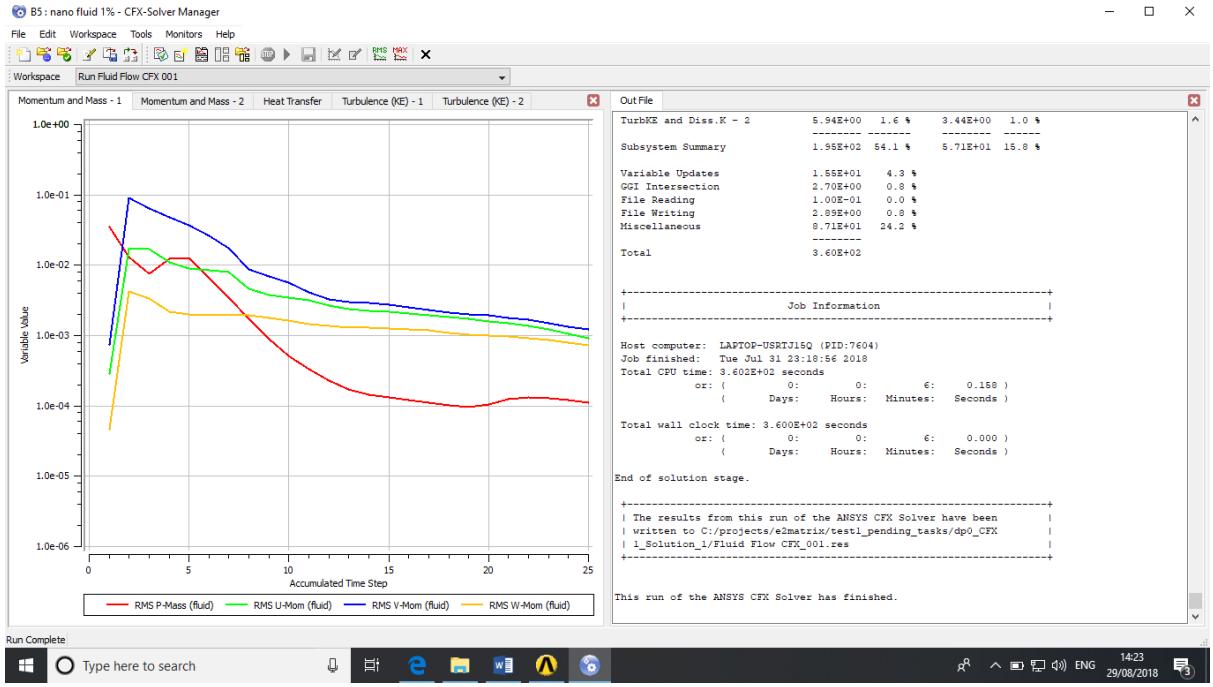

Fig. 5.17: RMS residual plots

5.4 Data Reduction

Efficacy of a HE is measured by comparing amount of heat that has been transported to the maximum amount feasible. It's a measure of how well a heat exchanger does at transferring heat from one fluid to another. Heat exchanger installation feasibility may be determined by this metric.

$$\text{Effectiveness} = Q_{actual}/Q_{max\ possible}$$

$$\varepsilon = m_c C_{pc} (T_{co} - T_{ci})/ C_{min} (T_{hi} - T_{ci}) = C_c (T_{co} - T_{ci})/ C_{min} (T_{hi} - T_{ci}) \quad (5.1)$$

CHAPTER-6

RESULTS AND DISCUSSION

ANSYS CFX 14.0 version is used for the CFD study, and velocity and temperature charts for several fluids are retrieved. The study includes six alternative combinations of base fluids and nanofluids in each of the six situations. For each individual, the efficiency of the heat exchanger is evaluated mathematically.

CASE 1: In this situation, the basic fluid is water. The properties are shown in table 6.1.

Table 6.1: Base fluid water for both hot & cold

FLUID TYPE	MASS FLOW RATE (Kg/s)	SPECIFIC HEAT (J/Kg K)
COLD FLUID	.05	4179.725
HOT FLUID	.04	4197.178

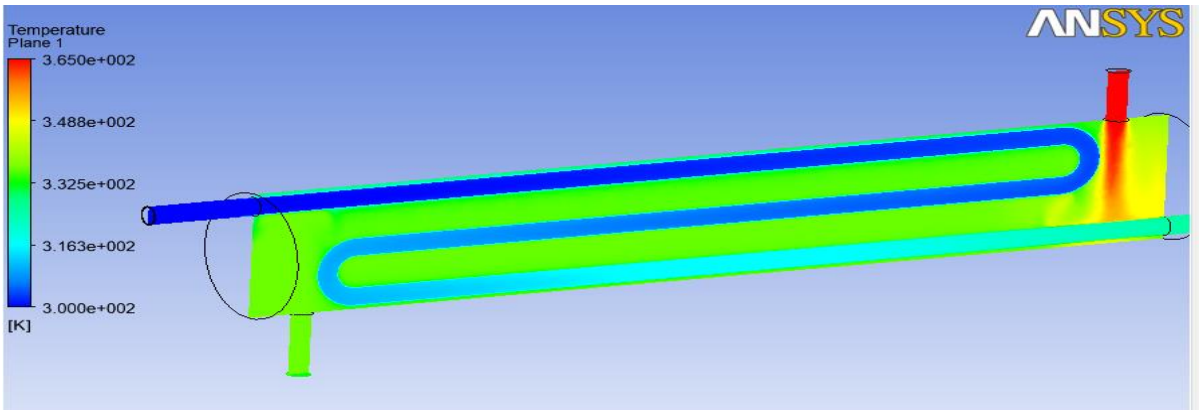

Fig. 6.1: Temperature contour using water as fluid

On the top right section of this temperature contour, we see a dark red hue signifying the presence of heated fluid, which drops in temperature as we travel left. Fluid entering the tube is represented in dark blue colour, while fluid exiting the tube is indicated in light blue colour (tube domain).

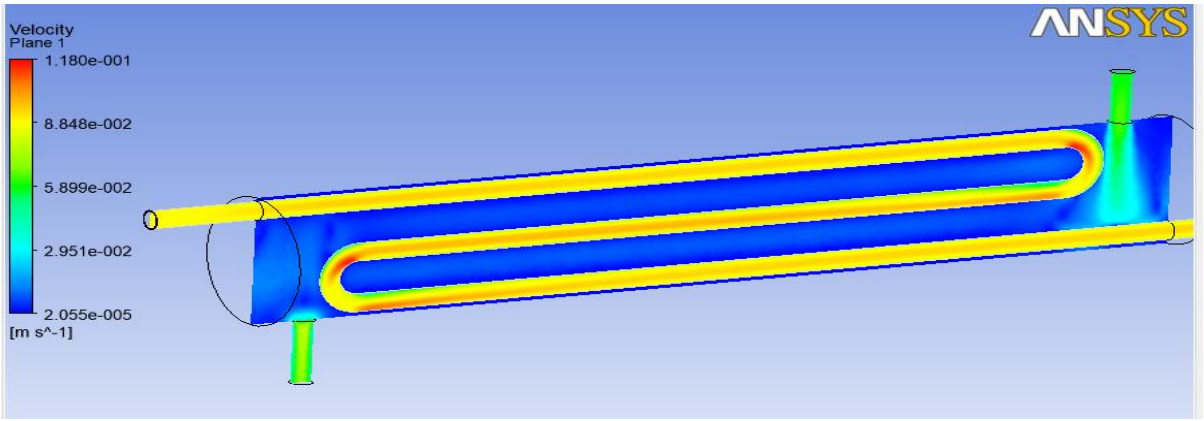

Fig. 6.2: Velocity contour using water as fluid

The velocity profile displayed above indicates a large magnitude at the entrance and a drop in magnitude as we go towards the shell's exit, which is depicted in green. A little increase in velocity occurs at U-tube bends because to centrifugal forces.

Table 6.2: Data on temperature output using water as a fluid

COLD FLUID IN	300K
COLD FLUID OUT	326.83K
HOT FLUID IN	365K
HOT FLUID OUT	334.9K

Effectiveness Calculation

Heat capacity of cold fluid, Cc = mc * Cpc = 0.05*4179.725 = 208.98 W/K

Heat capacity of hot fluid, Ch = mh * Cph =0.04*4197.178 = 167.887 W/K

Ch < Cc, Cmin = Ch Effectiveness,

Effectiveness = $C_C (T_{co}-T_{ci})/ C_h (T_{hi}-T_{ci})$

= 208.98*26.83/167.88*65=.513

CASE 2 : CuO/water nano fluid 1%

Table 6.3: Base fluid water for cold and hot fluid is CuO/water nano fluid 1%

FLUID TYPE	MASS FLOW RATE (Kg/s)	SPECIFIC HEAT (J/Kg K)
COLD FLUID	.05	4179.725
HOT FLUID	.04	4154.7

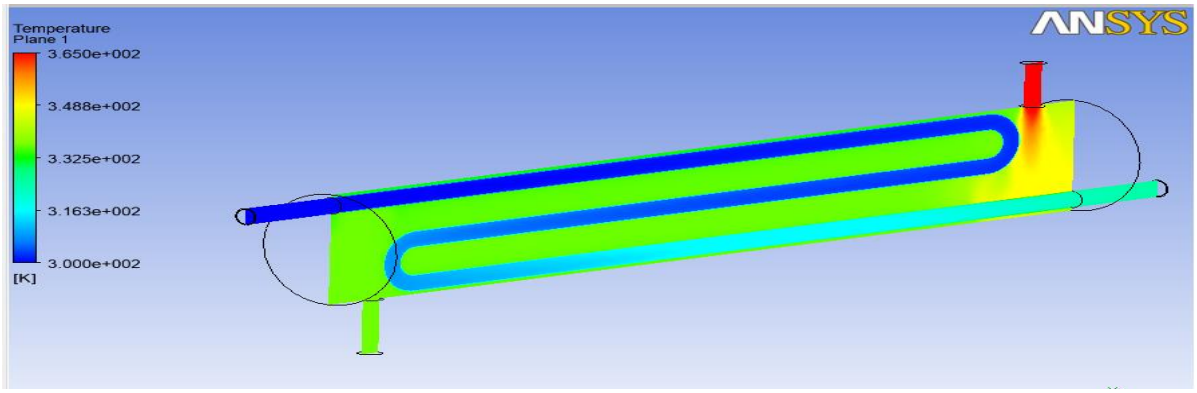

Fig. 6.3: Temperature contour for CuO/water nano fluid 1%

Fig 6.3 shows the temperature contour above the heated fluid entering the shell, with the top right region of the contour showing a dark red hue, and the temp of hot fluid decreasing as we travel to the left. Fluid entering the tube is represented in dark blue colour, while fluid exiting the tube is indicated in light blue colour (tube domain).

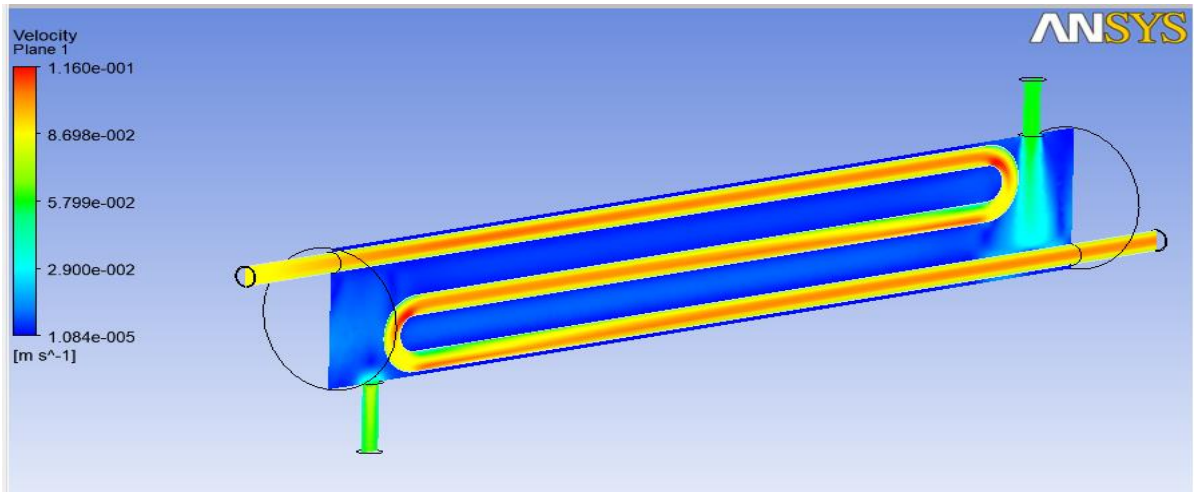

Fig. 6.4: Velocity contour for CuO/water nano fluid 1%

The velocity profile displayed above indicates a large magnitude at the entrance and a drop in magnitude as we go towards the shell's exit, which is depicted in green. A little increase in velocity occurs at U-tube bends because to centrifugal forces.

Table 6.4: Temperature output data for 1% CuO/water nano fluid

COLD FLUID IN	300K
COLD FLUID OUT	327.51K
HOT FLUID IN	365K
HOT FLUID OUT	335.8K

Effectiveness Calculation

Heat capacity of cold fluid, Cc = mc * Cpc = 0.05* 4179.7 = 208.98 W/K

Heat capacity of hot fluid, Ch = mh * Cph =0.04*4154.7 = 166.18W/K

Ch < Cc, Cmin = Ch Effectiveness,

Effectiveness = $C_C (T_{co}-T_{ci})/ C_h (T_{hi}-T_{ci})$

= 208.98*27.5/166.18*65= .532

CASE 3 : CuO/water nano fluid 2%

Table 6.5: Base fluid water for cold and hot fluid is CuO/water nano fluid 2%

FLUID TYPE	MASS FLOW RATE (Kg/s)	SPECIFIC HEAT (J/Kg K)
COLD FLUID	.05	4179.725
HOT FLUID	.04	4120.5

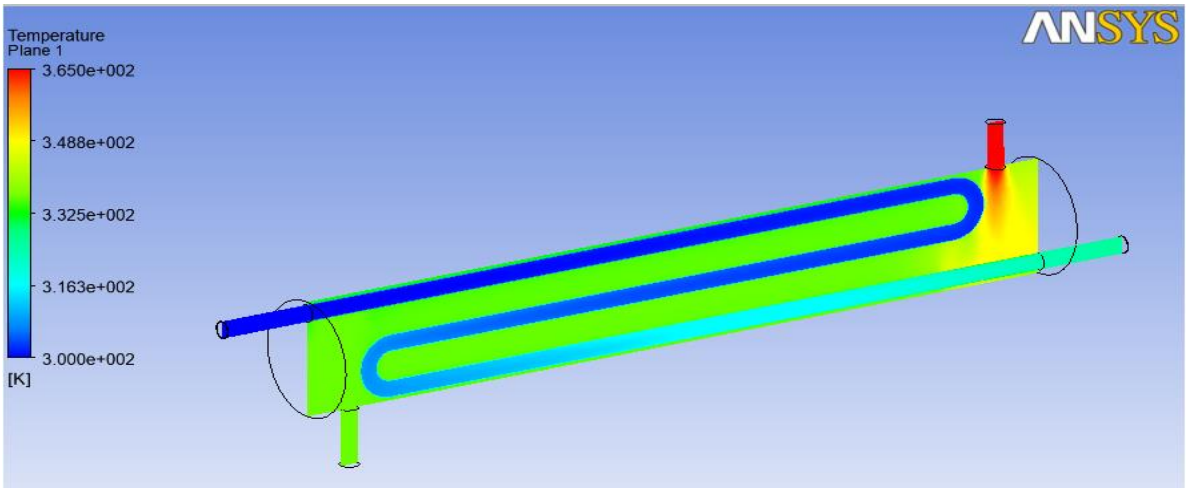

Fig. 6.5: Temperature contour for CuO/water nano fluid 2%

As we go leftward from the shell, the temperature profile given in fig. 6.5 shows a reduction in temperature of hot fluid as it enters shell. Fluid entering tube is represented in dark blue colour, while fluid exiting the tube is indicated in light blue colour (tube domain).

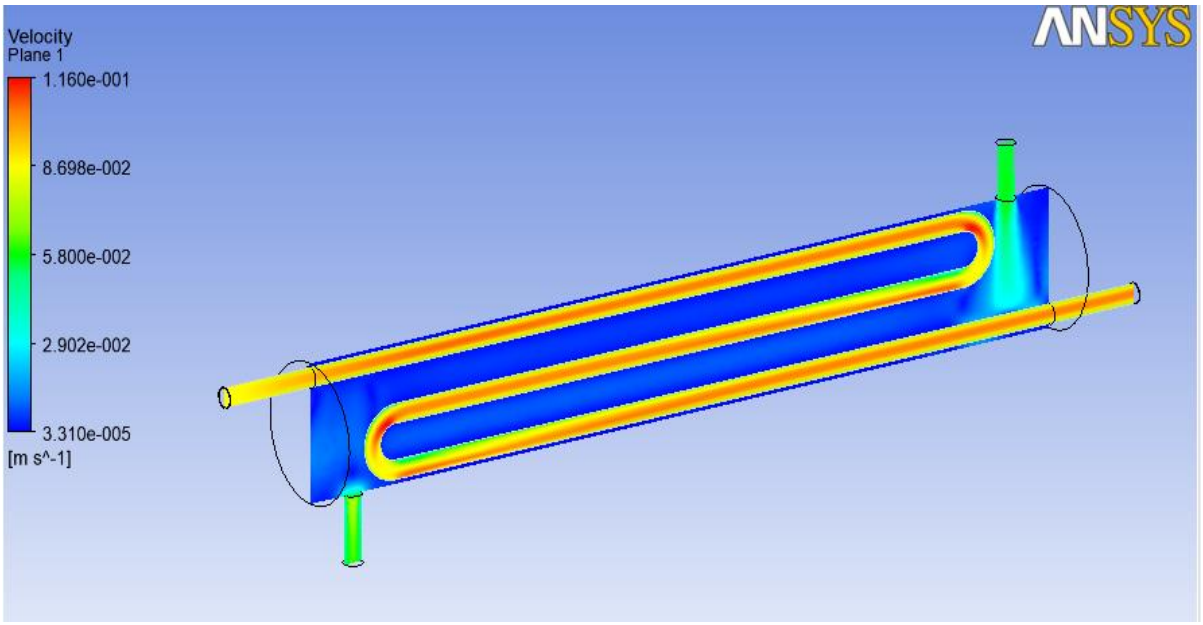

Fig. 6.6: Velocity contour for CuO/water nano fluid 2%

The velocity profile displayed above indicates a large magnitude at the entrance and a drop in magnitude as we go towards the shell's exit, which is depicted in green. A little increase in velocity occurs at U-tube bends because to centrifugal forces.

Table 6.6: CuO/water nano fluid with a 2% concentration of CuO

COLD FLUID IN	300K
COLD FLUID OUT	327.52K
HOT FLUID IN	365K
HOT FLUID OUT	335.8K

Effectiveness Calculation

Heat capacity of cold fluid, Cc = mc * Cpc = 0.05* 4179.7 = 208.98 W/K

Heat capacity of hot fluid, Ch = mh * Cph =0.04*4120.5 = 164.82W/K

Ch < Cc, Cmin = Ch Effectiveness,

Effectiveness = C_C (T_{co}-T_{ci})/ C_h (T_{hi}-T_{ci})

= 208.98*27.5/164.82*65= .536

CASE 4: CuO/water nano fluid 3%

Table 6.7: Base fluid water for cold and hot fluid is CuO/water nano fluid 3%

FLUID TYPE	MASS FLOW RATE (Kg/s)	SPECIFIC HEAT (J/Kg K)
COLD FLUID	.05	4179.725
HOT FLUID	.04	4086.2

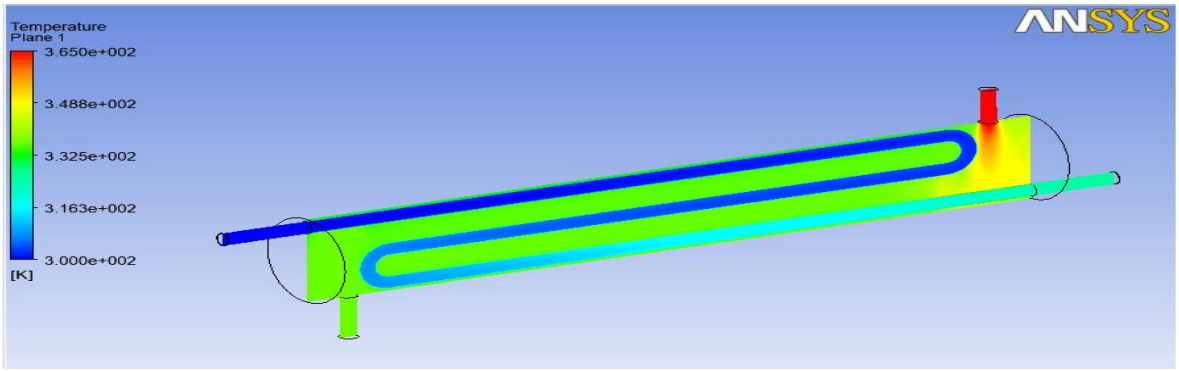

Fig. 6.7: Temperature contour for CuO/water nano fluid 3%

Fig 6.7 shows the temperature contour above heated fluid entering shell, which has a dark red hue on the top right side of contour & temp of hot fluid falls as we travel left of the shell. Fluid entering tube is represented in dark blue colour, while fluid exiting the tube is indicated in light blue colour (tube domain).

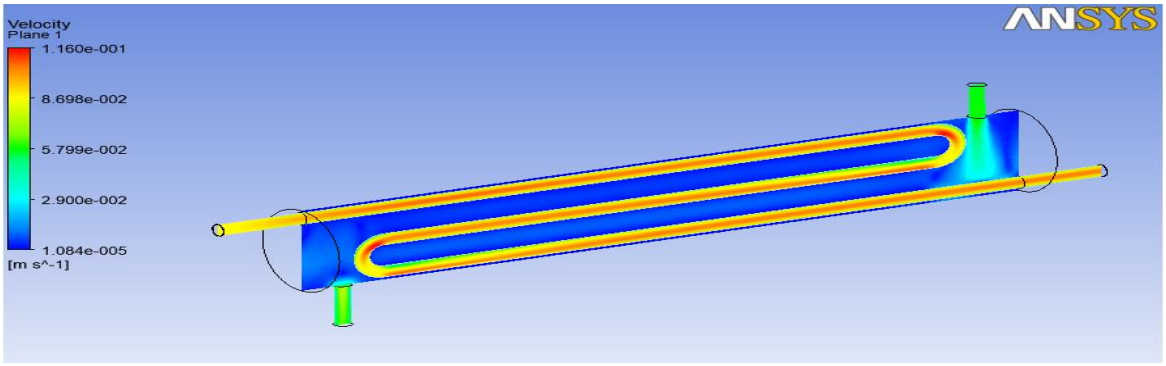

Fig. 6.8: Velocity contour for CuO/water nano fluid 3%

The velocity profile displayed above indicates a large magnitude at the entrance and a drop in magnitude as we go towards the shell's exit, which is depicted in green. A little increase in velocity occurs at U-tube bends because to centrifugal forces.

Table 6.8: A 3 percent CuO/water nanofluid was used to measure the temperature.

COLD FLUID IN	300K
COLD FLUID OUT	327.56K
HOT FLUID IN	365K
HOT FLUID OUT	335.8K

Effectiveness Calculation

Heat capacity of cold fluid, Cc = mc * Cpc = 0.05* 4179.7 = 208.98 W/K

Heat capacity of hot fluid, Ch = mh * Cph =0.04*4086.2 = 163.44 W/K

Ch < Cc, Cmin = Ch Effectiveness,

Effectiveness = $C_C (T_{co}-T_{ci})/ C_h (T_{hi}-T_{ci})$

= 207.54*27.5/163.44*65=.537

CASE 5 : CuO/water nano fluid 4%

Table 6.9: Base fluid water for cold and hot fluid is CuO/water nano fluid 4%

FLUID TYPE	MASS FLOW RATE (Kg/s)	SPECIFIC HEAT (J/Kg K)
COLD FLUID	.05	4179.725
HOT FLUID	.04	4052

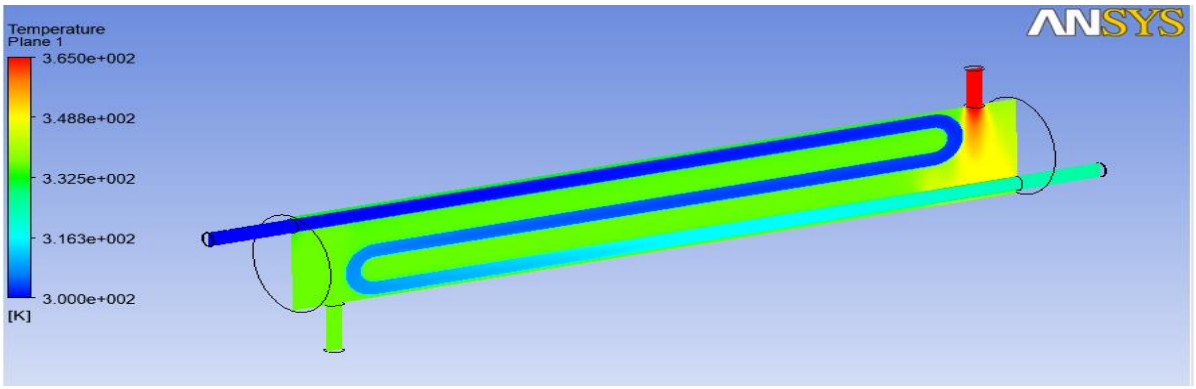

Fig. 6.9: Temperature contour for CuO/water nano fluid 4%

FIG. 6.9 depicts the temperature profile of heated fluid entering a shell, with the top right region of the graph showing a dark red hue, while the lower left half shows a decreasing temperature profile. Fluid entering the tube is represented in dark blue colour, while fluid exiting the tube is indicated in light blue colour (tube domain).

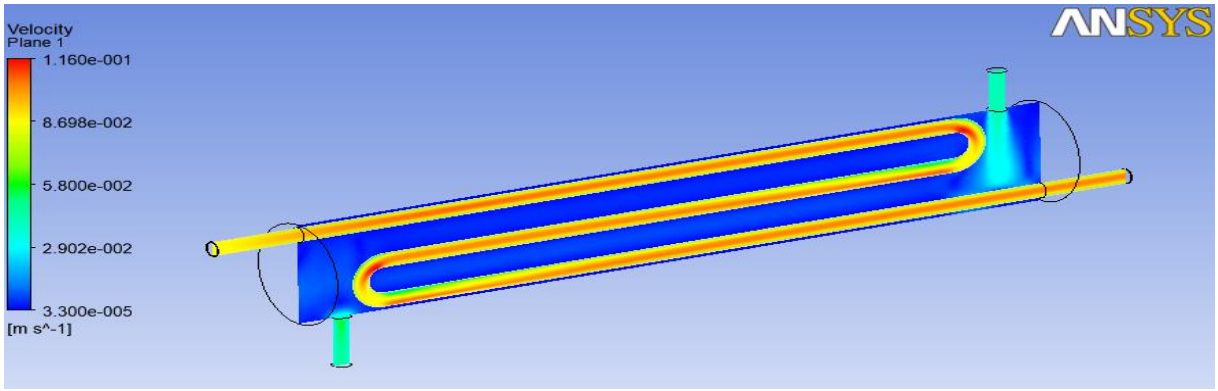

Fig. 6.10: Velocity contour for CuO/water nano fluid 4%

The velocity profile displayed above indicates a large magnitude at the entrance and a drop in magnitude as we go towards the shell's exit, which is depicted in green. A little increase in velocity occurs at U-tube bends because to centrifugal forces.

Table 6.10: CuO/water nanofluid 4 percent's temperature output data

COLD FLUID IN	300K
COLD FLUID OUT	327.53K
HOT FLUID IN	365K
HOT FLUID OUT	335.8K

Effectiveness Calculation

Heat capacity of cold fluid, Cc = mc * Cpc = 0.05* 4179.7 = 208.98 W/K

Heat capacity of hot fluid, Ch = mh * Cph =0.04*4052 = 162.08 W/K

Ch < Cc, Cmin = Ch Effectiveness,

Effectiveness = C_C (T_{co}-T_{ci})/ C_h (T_{hi}-T_{ci})

= 208.98 * 27.53/162.08 * 65=.546

CASE 6 : CuO/water nano fluid 5%

Table 6.11: Base fluid water for cold and hot fluid is CuO/water nano fluid 5%

FLUID TYPE	MASS FLOW RATE (Kg/s)	SPECIFIC HEAT (J/Kg K)
COLD FLUID	.05	4179.725
HOT FLUID	.04	4017.8

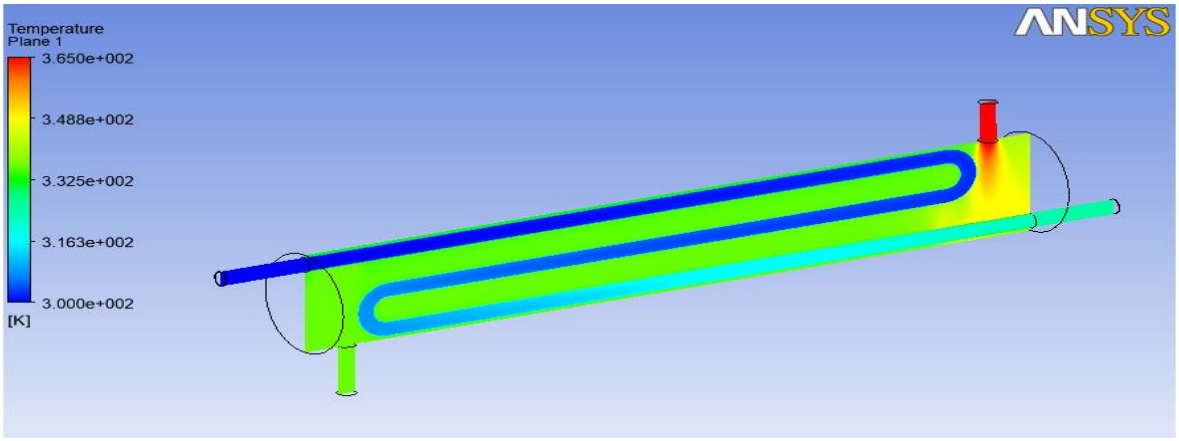

Fig. 6.11: Temperature contour for CuO/water nano fluid 5%

Fig 6.11 shows the temperature contour above heated fluid entering the shell, with the top right region of the contour showing a dark red hue, and temp of hot fluid decreasing as we travel to the left. Fluid entering tube is represented in dark blue colour, while fluid exiting the tube is indicated in light blue colour (tube domain).

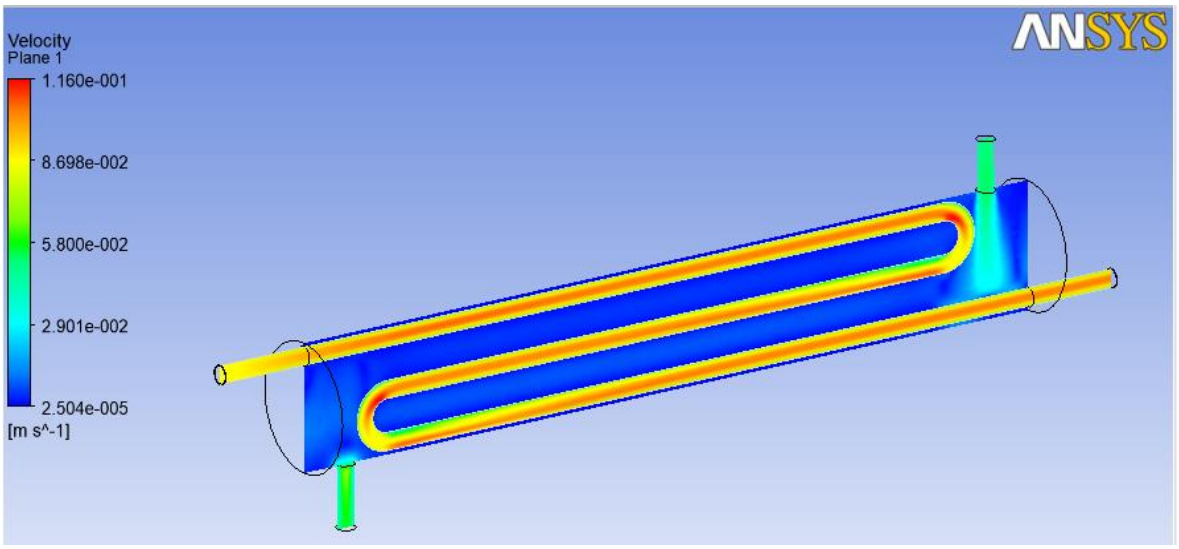

Fig. 6.12: Velocity contour for CuO/water nano fluid 5%

The velocity profile displayed above indicates a large magnitude at the entrance and a drop in magnitude as we go towards the shell's exit, which is depicted in green. A little increase in velocity occurs at U-tube bends because to centrifugal forces.

Table 6.12: CuO/Water Nano Fluid 5 Percent Temperature Output Data

COLD FLUID IN	300K
COLD FLUID OUT	327.54K
HOT FLUID IN	365K
HOT FLUID OUT	335.8K

Effectiveness Calculation

Heat capacity of cold fluid, $Cc = mc * Cpc = 0.05 * 4179.7 = 208.98$ W/K

Heat capacity of hot fluid, $Ch = mh * Cph = 0.04 * 3998 = 159.92$ W/K

$Ch < Cc$, $Cmin = Ch$ Effectiveness,

Effectiveness $= Cc (T_{co}-T_{ci}) / Ch (T_{hi}-T_{ci})$

$= 207.54 * 27.5 / 159.92 * 65 = .549$

Effectiveness is estimated for various percentages of nano fluids after doing CFD study on shell & serpentine heat exchangers by CFX solver. Different nano fluid compositions are shown in a table below 6.13.

Table 6.13: CuO/Water Nano Fluid Effectiveness in Different Compositions

FLUID	EFFECTIVENESS
WATER	0.513
NANO FLUID 1%	0.532
NANO FLUID 2%	0.536
NANO FLUID 3%	0.537
NANO FLUID 4%	0.546
NANO FLUID 5%	0.549

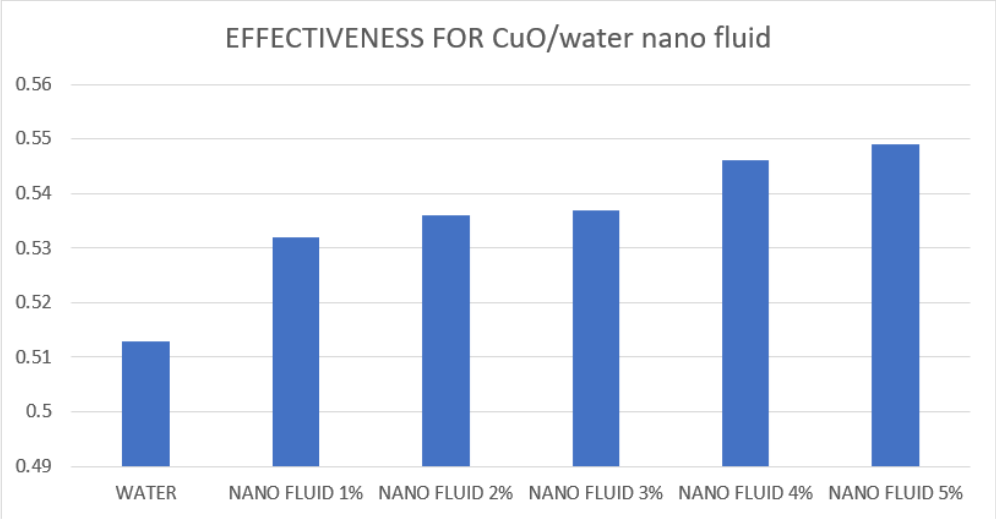

Fig. 6.13: Comparison of the effectiveness of nano fluids with varied compositions of CuO and water.

CASE 7: Al_2O_3/water nano fluid 1%

Table 6.14: Base fluid water for cold and hot fluid is Al_2O_3/water nano fluid 1%

FLUID TYPE	MASS FLOW RATE (Kg/s)	SPECIFIC HEAT (J/Kg K)
COLD FLUID	.05	4179.725
HOT FLUID	.04	4150.9

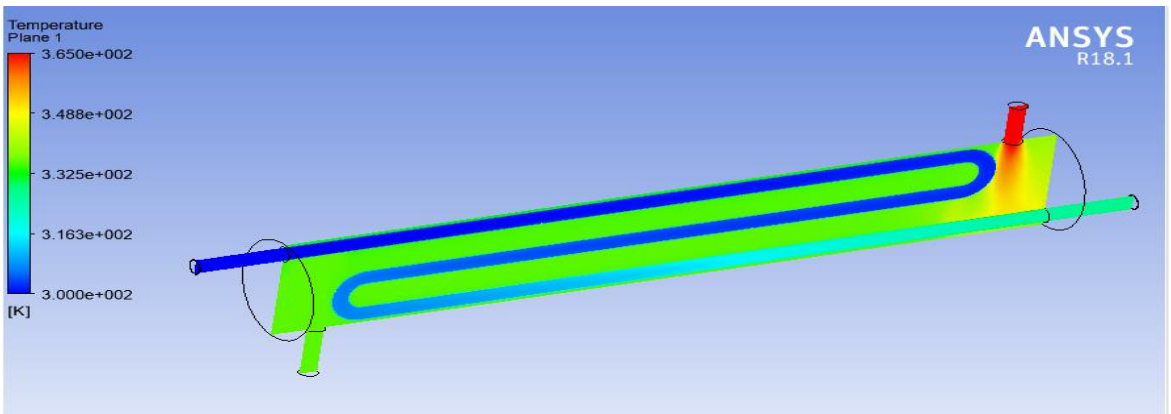

Fig. 6.14: Temperature contour for Al_2O_3/water nano fluid 1%

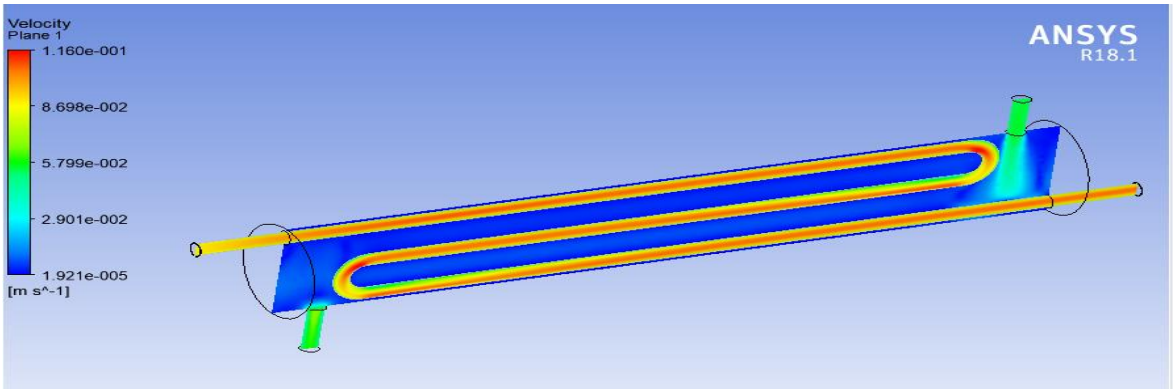

Fig. 6.15: Velocity contour for Al_2O_3/water nano fluid 1%

Table 6.15: Temperature output data for Al_2O_3/water nano fluid 1%

COLD FLUID IN	300K
COLD FLUID OUT	327.51K
HOT FLUID IN	365K
HOT FLUID OUT	335.86K

Effectiveness Calculation

Heat capacity of cold fluid, Cc = mc * Cpc = 0.05* 4179.7 = 208.98 W/K

Heat capacity of hot fluid, Ch = mh * Cph =0.04*4150.9 = 166.036 W/K

Ch < Cc, Cmin = Ch Effectiveness,

Effectiveness = Cc (T_{co}-T_{ci})/ Ch (T_{hi}-T_{ci})

= 208.98*27.5/166.036*65=.5325

CASE 8 : Al_2O_3/water nano fluid 2%

Table 6.16: Base fluid water for cold and hot fluid is Al_2O_3/water nano fluid 2%

FLUID TYPE	MASS FLOW RATE (Kg/s)	SPECIFIC HEAT (J/Kg K)
COLD FLUID	.05	4179.725
HOT FLUID	.04	4112.8

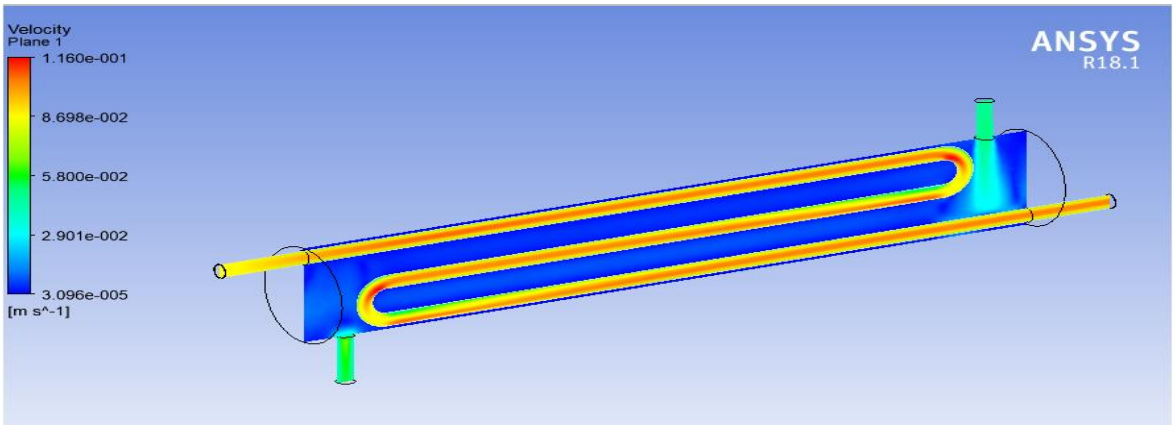

Fig. 6.16: Velocity contour for Al_2O_3/water nano fluid 2%

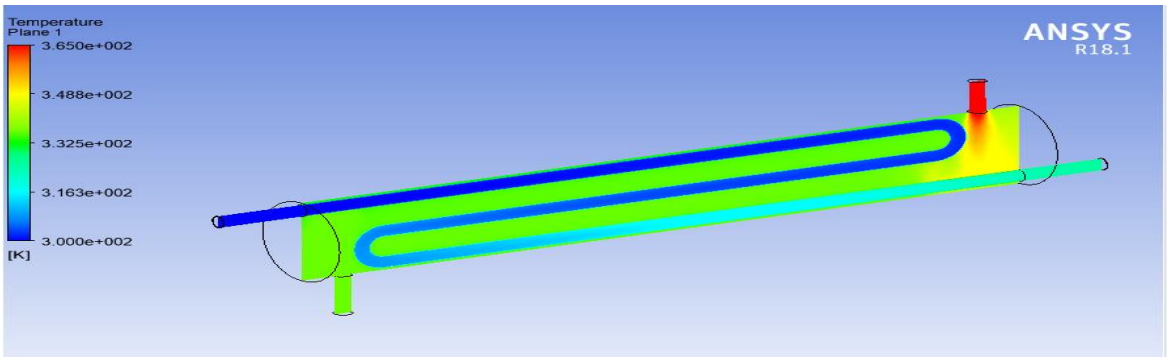

Fig. 6.17: Temperature contour for Al_2O_3/water nano fluid 2%

Table 6.17: Temperature output data for Al_2O_3/water nano fluid 2%

COLD FLUID IN	300K
COLD FLUID OUT	327.52K
HOT FLUID IN	365K
HOT FLUID OUT	335.87K

Calculation of Efficacy

Heat capacity of cold fluid, Cc = mc * Cpc = 0.05* 4179.7 = 208.98 W/K

Heat capacity of hot fluid, Ch = mh * Cph =0.04*4112.8 = 164.512 W/K

Ch < Cc, Cmin = Ch Effectiveness,

Effectiveness = Cc (Tco-Tci)/ Ch (Thi-Tci)

= 208.98*27.52/164.512*65=.5378

CASE 9: Al_2O_3/water nano fluid 3%

Table 6.18: Base fluid water for cold and hot fluid is Al_2O_3/water nano fluid 3%

FLUID TYPE	MASS FLOW RATE (Kg/s)	SPECIFIC HEAT (J/Kg K)
COLD FLUID	.05	4179.725
HOT FLUID	.04	4074.8

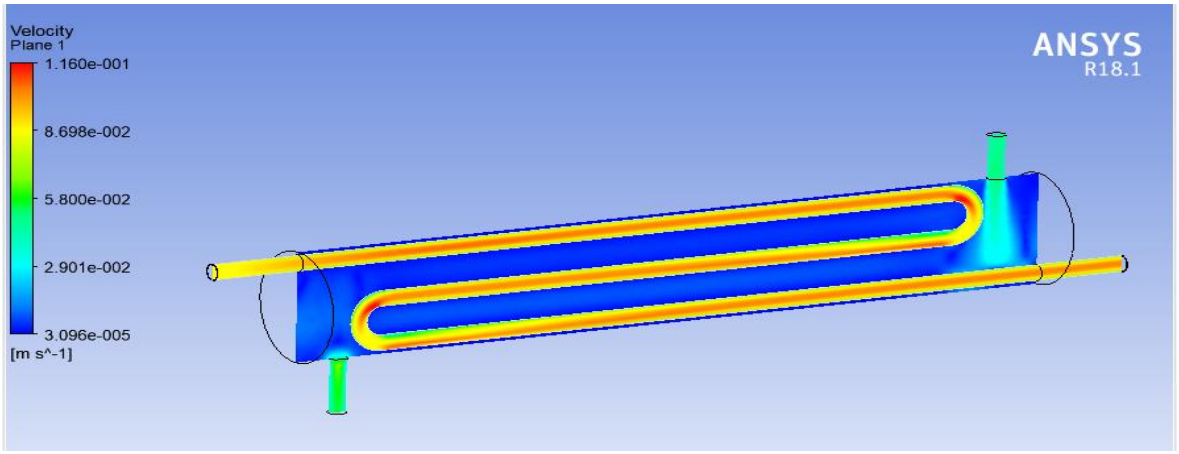

Fig. 6.18: Velocity contour for Al_2O_3/water nano fluid 3%

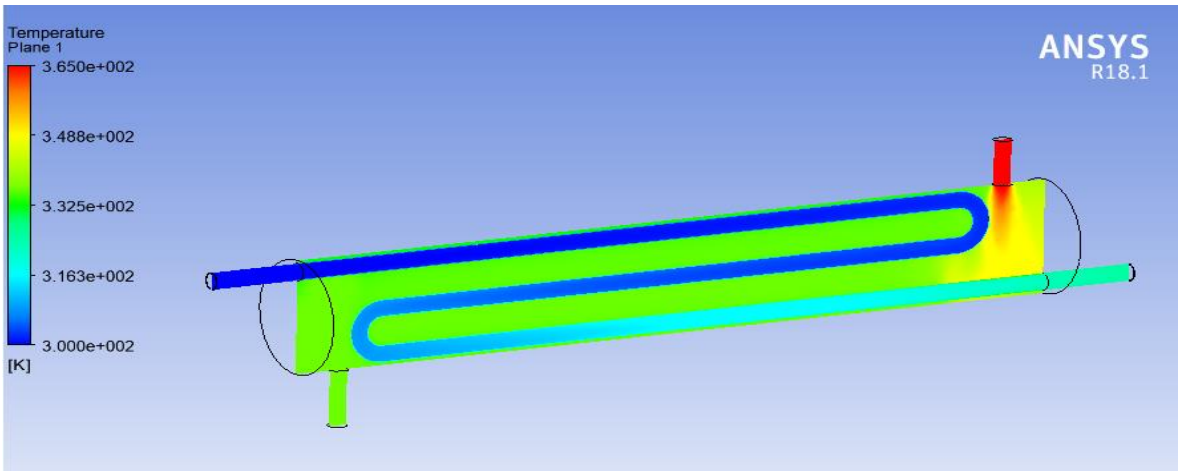

Fig. 6.19: Temperature contour for Al_2O_3/water nano fluid 3%

Table 6.19: Temperature output data for Al_2O_3/water nano fluid 3%

COLD FLUID IN	300K
COLD FLUID OUT	327.529K
HOT FLUID IN	365K
HOT FLUID OUT	335.88K

Calculation of Efficacy

Heat capacity of cold fluid, $C_c = m_c * C_{pc} = 0.05 * 4179.7 = 208.98$ W/K

Heat capacity of hot fluid, $C_h = m_h * C_{ph} = 0.04 * 4074.8 = 162.992$ W/K

$C_h < C_c$, $C_{min} = C_h$ Effectiveness,

Effectiveness $= C_c (T_{co}-T_{ci}) / C_h (T_{hi}-T_{ci})$

$= 208.98 * 27.52 / 162.992 * 65 = .5428$

CASE 10 : Al_2O_3/water nano fluid 4%

Table 6.20: Base fluid water for cold and hot fluid is Al_2O_3/water nano fluid 4%

FLUID TYPE	MASS FLOW RATE (Kg/s)	SPECIFIC HEAT (J/Kg K)
COLD FLUID	.05	4179.725
HOT FLUID	.04	4036.7

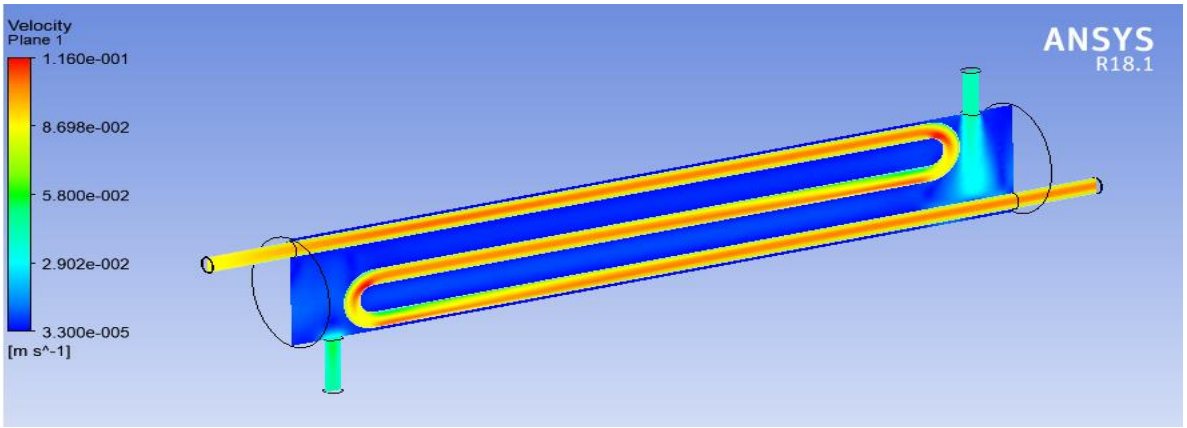

Fig. 6.20: Velocity contour for Al_2O_3/water nano fluid 4%

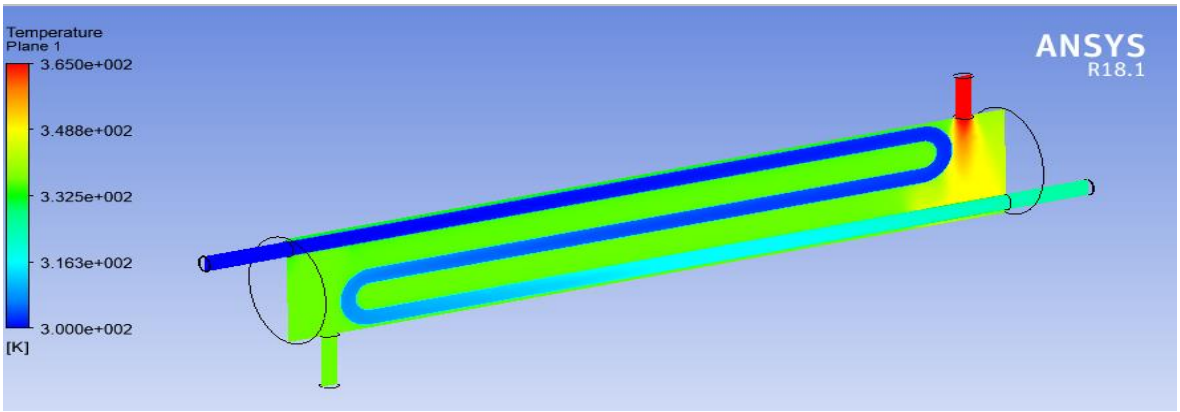

Fig. 6.21: Temperature contour for Al_2O_3/water nano fluid 4%

Table 6.21: Temperature output data for Al_2O_3/water nano fluid 4%

COLD FLUID IN	300K
COLD FLUID OUT	327.53K
HOT FLUID IN	365K
HOT FLUID OUT	335.88K

Calculation of Efficacy

Heat capacity of cold fluid, Cc = mc * Cpc = 0.05* 4179.7 = 208.98 W/K

Heat capacity of hot fluid, Ch = mh * Cph =0.04*4036.7 = 161.468 W/K

Ch < Cc, Cmin = Ch Effectiveness,

Effectiveness = Cc (T_{co}-T_{ci})/ Ch (T_{hi}-T_{ci})

= 208.98*27.52/161.468*65=.5479

CASE 11: Al_2O_3/water nano fluid 5%

Table 6.22: Base fluid water for cold and hot fluid is Al_2O_3/water nano fluid 5%

FLUID TYPE	MASS FLOW RATE (Kg/s)	SPECIFIC HEAT (J/Kg K)
COLD FLUID	.05	4179.725
HOT FLUID	.04	3998

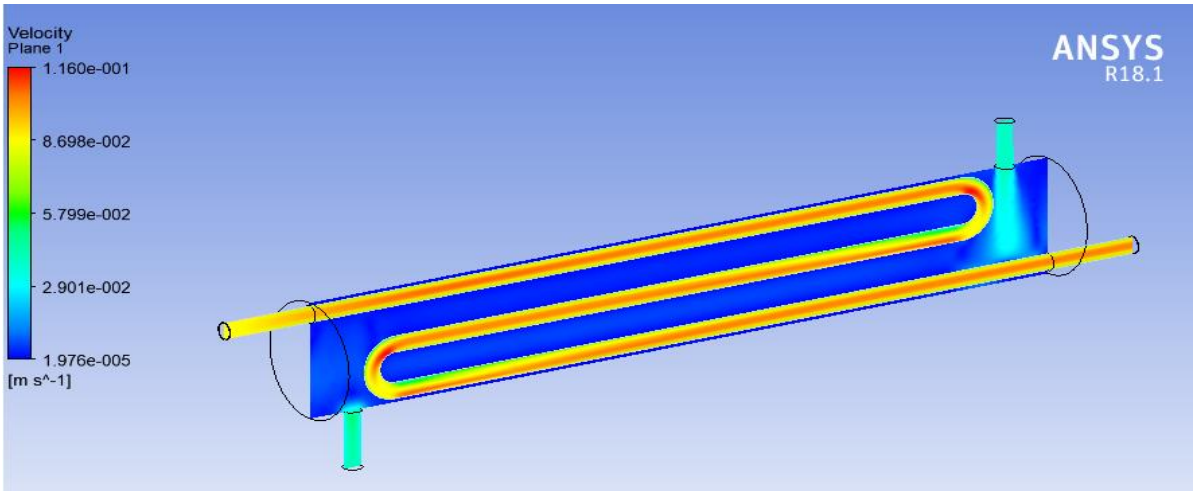

Fig. 6.22: Velocity contour for Al_2O_3/water nano fluid 5%

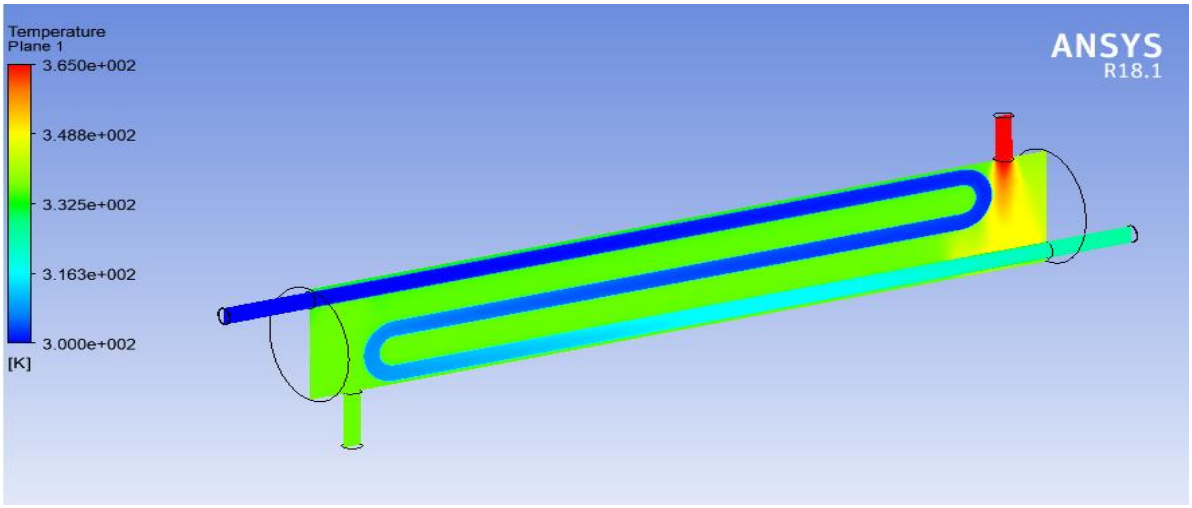

Fig. 6.23: Temperature contour for Al_2O_3/water nano fluid 5%

Table 6.23: Temperature output data for Al_2O_3/water nano fluid 5%

COLD FLUID IN	300K
COLD FLUID OUT	327.54K
HOT FLUID IN	365K
HOT FLUID OUT	335.88K

Calculation of Efficacy

Heat capacity of cold fluid, Cc = mc * Cpc = 0.05* 4179.7 = 208.98 W/K

Heat capacity of hot fluid, Ch = mh * Cph =0.04*3998 = 159.92 W/K

Ch < Cc, Cmin = Ch Effectiveness,

Effectiveness = Cc (Tco-Tci)/ Ch (Thi-Tci)

= 208.98*27.54/159.92 * 65=.5536

Table 6.24: Effectiveness for varied Al2O3/water nanofluid compositions

WATER	0.513
NANO FLUID 1%	0.5325
NANO FLUID 2%	0.5378
NANO FLUID 3%	0.5428
NANO FLUID 4%	0.5479
NANO FLUID 5%	0.5536

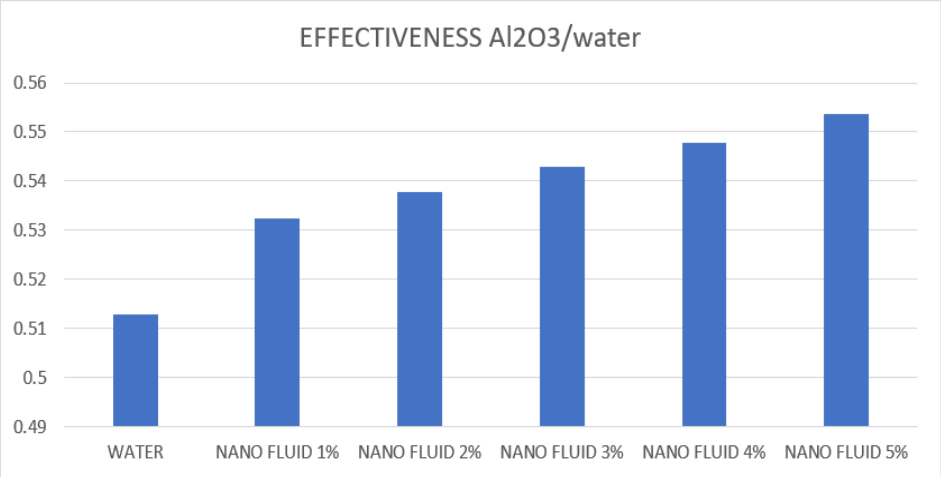

Fig. 6.24: Comparison of nanofluids with varied compositions of Al_2O_3/water

Fig. 6.25: comparative evaluation of impact Fluids with nanoparticles of Al_2O_3 and CuO

CHAPTER-7
CONCLUSION

7.1 Conclusion

In a base fluid like water, ethylene glycol, or oil, nanometric metallic or ceramic particles are suspended in a colloidal solution. Nanofluids may considerably enhance the HT properties of original fluid because of their enhanced thermal transport capabilities. It is possible to simulate the performance of both shell and serpentine heat exchangers using computational fluid dynamics (CFD) simulations using a wide range of particle concentrations of CuO and Al2O3. When the concentration of nanoparticles increases, the effectiveness value also increases. The numerical findings show that nanofluids have a significant increase in heat transmission compared to their base fluid. Heat transfer and efficiency are higher when Al2O3/water nano fluid is utilised for analysis than when CuO/water nano fluid is. This is why Al2O3/water nano fluid is the best choice.

As the concentration of nanoparticles rises, so does the rate of heat transmission. Nano fluids have a larger turbulence kinetic energy than water, resulting in increased heat transfer from turbulent flow.

1) The efficiency & cooling performance of a shell & serpentine HE may be improved by using nanofluids.
2) Due to minuscule volume fractions and ultra-fine particles of nanofluid, there is no additional pressure drop across serpentine heat exchangers when utilising this coolant.
3) Low-velocity flows are more affected by nanofluids, whereas high-velocity flows are less affected by nanofluids because the flow rate dominates.
4) The impact of nanofluids on boundary layer development is greatest near the entry area owing to the influence of solid particles.

7.2 Future Scope

A new type of fluid known as ion fluids necessitates research in improvement of HT rate and its possible application in HE. Also, usage of baffling with varying geometrical parameters of

shell and serpentine heat exchangers by various types of nano fluids and ion fluids could be envisaged to achieve better cooling characteristics.

REFERENCES

[1] Rao, Y., Li, B., Feng, Y., 2015. Heat transfer of turbulent flow over surfaces with spherical dimples and teardrop dimples. Exp. Therm Fluid Sci. 61, 201–209.

[2] Cabeza, L.F., de Gracia, A., Fernandez, A.I., et al., 2017. Supercritical CO2 as heat transfer fluid: A review. Appl. Therm. Eng. 125, 799–810.

[3] Ehsan, M.M., Guan, Z., Klimenko, A.Y., 2018. A comprehensive review on heat transfer and pressure drop characteristics and correlations with supercritical CO2 under heating and cooling applications. Renew. Sustain. Energy Rev. 92, 658–675.

[4] Baik, S., Kim, S.G., Lee, J., et al., 2017. Study on CO2 – water printed circuit heat exchanger performance operating under various CO2 phases for S-CO2 power cycle application. Appl. Therm. Eng. 113, 1536–1546.

[5] Ren, Z., Zhang, C.R., Jiang, P.X., et al., 2019. Investigation on local convection heat transfer of supercritical CO2 during cooling in horizontal semicircular channels of printed circuit heat exchanger. Appl. Therm. Eng. 157, 113697.

[6] Jiang, Y., Liese, E., Zitney, S.E., et al., 2018. Design and dynamic modeling of printed circuit heat exchangers for supercritical carbon dioxide brayton power cycles. Appl. Energy 231, 1019–1032.

[7] Marchionni, M., Chai, L., Bianchi, G., et al., 2019. Numerical modelling and transient analysis of a printed circuit heat exchanger used as recuperator for supercritical CO2 heat to power conversion systems. Appl. Therm. Eng. 161, 115190.

[8] Ma, T., Li, M.J., Xu, J.L., et al., 2019. Thermodynamic analysis and performance prediction on dynamic response characteristic of PCHE in 1000 MW S-CO2 coal fired power plant. Energy 175, 123–138.

[9] Guo, J., Huai, X., 2017. Performance analysis of printed circuit heat exchanger for supercritical carbon dioxide. ASME J. Heat Transfer 139, 061801.

[10] Li, X.H., Deng, T.R., Ma, T., et al., 2019. A new evaluation method for overall heat transfer performance of supercritical carbon dioxide in a printed circuit heat exchanger. Energy Convers. Manage. 193, 99–105.

[11] Arora, B. B., Kumar, M., & Maji, S. (2010). Study of inlet conditions on diffuser performance. International Journal of Theoretical and applied Mechanics, 5(2), 201-221.

[12] Eter, A., Groeneveld, D., Tavoularis, S., 2017. Convective heat transfer in supercritical flows of CO2 in tubes with and without flow obstacles. Nucl. Eng. Des. 313, 162–176.

[13] Nascimento, I.P., Garcia, E.C., 2016. Heat transfer performance enhancement in compact heat exchangers by using shallow square dimples in flat tubes. Appl. Therm. Eng. 96, 659–670.

[14] Manoram, R.B., Moorthy, R.S., Ragunathan, R., 2020. Investigation on infuence of dimpled surfaces on heat transfer enhancement and friction factor in solar water heater. J. Therm. Anal. Calorim. 1–18. http://dx.doi.org/10.1007/ s10973-020-09746-0.

[15] Sahu, M.K., Prasad, R.K., 2017. Thermohydraulic performance analysis of an arc shape wire roughened solar air heater. Renew. Energy 198, 598–614.

[16] Thangamuthu, T., Rathanasamy, R., Kulandaivelu, S., et al., 2020. Experimental investigation on the influence of carbon-based nanoparticle coating on the heat transfer characteristics of the microprocessor. J. Compos. Mater. 54 (1), 61–70

[17] Bonanno, A., Raimondo, M., Pinelli, M., 2019. Use of nanostructured coating to improve heat exchanger efficiency. In: Tolio, T., Copani, G., Terkaj, W. (Eds.), Factories of the Future. Springer, Cham, http://dx.doi.org/10.1007/978- 3-319-94358-9_13.

[18] Meikandan, M., Malarmohan, K., Hemachandran, E., 2019. Experimental investigation on thermal performance of nanocoated surfaces for air-conditioning applications. Therm. Sci. 23 (2A), 457–463.

[19] Kumar, N., Britto, P.N., Richaredsion, B., 2020b. Design and analysis of heat exchanger with nano coating. Int. Res. J. Eng. Technol. 7 (4), 294–298.

[20] Arora, B. B., & Pathak, B. D. (2011). CFD analysis of axial annular diffuser with both hub and casing diverging at unequal angles. International Journal of Dynamics of Fluids, 7(1),109+. https://link.gale.com/apps/doc/A323658331/AONE?u=anon~c01943e7&sid=googleScholar&xid=b235dc53

[21] Ali, R.K., Sharafeldeen, M.A., Berbish, N.S., et al., 2016. Convective heat transfer enhancement inside tubes using inserted helical coils. Therm. Eng. 63 (1), 42–50.

[22] Jadhav, M., Awari, R., Bibe, D., et al., 2016. Review on enhancement of heat transfer by active method. Int. J. Curr. Eng. Technol. 6 (6), 221–226.

[23] Chai, L., Tassou, S.A., 2018. A review of airside heat transfer augmentation with vortex generators on heat transfer surface. Energies 11, 2737.

[24] Hardial Singh and B.B. Arora 2021 *IOP Conf. Ser.: Mater. Sci. Eng.* **1168** 012029

[25] Bacellar, D., Aute, V., Huang, Z.W., et al., 2017. Design optimization and validation of high-performance heat exchangers using approximation assisted optimization and additive manufacturing. Sci. Technol. Built Environ. 23 (6), 896–911

[26] Yu, C., Xue, X., Shi, X., et al., 2021. A three-dimensional numerical and multiobjective optimal design of wavy plate-fins heat exchangers. ProcesManses 9 (9), 1–18

[27] Shi, H.N., Ma, T., Chu, W.X., et al., 2017. Optimization of inlet part of a microchannel ceramic heat exchanger using surrogate model coupled with genetic algorithm. Energy Convers. Manage. 149, 988–996.

[28] Lei, X.S., Shuang, J.J., Yang, P., et al., 2019. Parametric study and optimization of dimpled tubes based on Response Surface Methodology and desirability approach. Int. J. Heat Mass Transfer 142, 118453.

[29] Baadache, K., Bougriou, C., 2015. Optimisation of the design of shell and double concentric tubes heat exchanger using the Genetic Algorithm. Heat Mass Transfer 51, 1371–1381.

[30] Khosravi, R., Khosravi, A., Nahavandi, S., et al., 2015. Effectiveness of evolutionary algorithms for optimization of heat exchangers. Energy Convers. Manage. 89, 281–288.

[31] Sadeghzadeh, H., Ehyaei, M.A., Rosen, M.A., 2015. Techno-economic optimization of a shell and tube heat exchanger by genetic and particle swarm algorithms. Energy Convers. Manage. 93, 84–91.

[32] John, A.K., Krishnakumar, K., 2017. Performing multiobjective optimization on perforated plate matrix heat exchanger surfaces using genetic algorithm. Int. J. Simul. Multidiscip. Des. Optim. 8, 1–8.

[33] Imran, M., Pambudi, N.A., Farooq, M., 2017. Thermal and hydraulic optimization of plate heat exchanger using multi objective genetic algorithm. Case Stud. Therm. Eng. 10, 570–578.

[34] Tharakeshwar, T.K., Seetharamu, K.N., Prasa, B.D., 2017. Multi-objective optimization using bat algorithm for shell and tube heat exchangers. Appl. Therm. Eng. 110, 1029–1038.

[35] Aasi, H.K., Mishra, M., 2020. Detailed design optimization of three-fluid parallel flow plate-fin heat exchanger using second law analysis. ASME J. Heat Transfer 142, 081901.